

REVIEW ARTICLE

[View Article Online](#)
[View Journal](#) | [View Issue](#)

Cite this: *Chem. Soc. Rev.*, 2013,
42, 2039

Organic sensitizers from D- π -A to D-A- π -A: effect of the internal electron-withdrawing units on molecular absorption, energy levels and photovoltaic performances

Yongzhen Wu and Weihong Zhu*

The high performance and low cost of dye-sensitized solar cells (DSSCs) have drawn great interest from both academic and industrial circles. The research on exploring novel efficient sensitizers, especially on inexpensive metal-free pure organic dyes, has never been suspended. The donor- π bridge–acceptor (D- π -A) configuration is mainstream in the design of organic sensitizers due to its convenient modulation of the intramolecular charge-transfer nature. Recently, it has been found that incorporation of additional electron-withdrawing units (such as benzothiadiazole, benzotriazole, quinoxaline, phthalimide, diketopyrrolopyrrole, thienopyrazine, thiazole, triazine, cyanovinyl, cyano- and fluoro-substituted phenyl) into the π bridge as internal acceptors, termed the D-A- π -A configuration, displays several advantages such as tuning of the molecular energy levels, red-shift of the charge-transfer absorption band, and distinct improvement of photovoltaic performance and stability. We apply the D-A- π -A concept broadly to the organic sensitizers containing additional electron-withdrawing units between electron donors and acceptors. This review is projected to summarize the category of pure organic sensitizers on the basis of the D-A- π -A feature. By comparing the structure–property relationship of typical photovoltaic D-A- π -A dyes, the important guidelines in the design of such materials are highlighted.

Received 20th August 2012

DOI: 10.1039/c2cs35346f

www.rsc.org/csr

Shanghai Key Laboratory of Functional Materials Chemistry, Key Laboratory for Advanced Materials and Institute of Fine Chemicals, East China University of Science and Technology, Shanghai 200237, P. R. China.
E-mail: whzhu@ecust.edu.cn; Fax: +86 21-6425-2758



Yongzhen Wu is a graduate student pursuing a PhD under the supervision of Prof. Weihong Zhu at East China University of Science and Technology (ECUST). He received his BA in Applied Chemistry from ECUST in 2008. His PhD research is focused on the synthesis of pure metal-free organic sensitizers for dye-sensitized solar cells (DSSCs).

Yongzhen Wu

Introduction

Energy is the initial driving force for human society advancement. Especially, human society has made great progress due



Weihong Zhu

Prof. Weihong Zhu received his PhD degree in 1999 from East China University of Science and Technology (ECUST), China. He worked in AIST Central 5, Tsukuba, Japan (postdoctoral) from 2001 to 2003 and worked in Tsukuba University, Japan (visiting professor) from 2004 to 2005. He became a full professor in 2004 and deputy director in 2006. He is co-inventor of 20 Chinese Invention Patents (13 authorized) and has published

106 peer-reviewed papers. His current research interests are focused on functional chromophores, including fluorescent sensors, photochromism and metal-free organic sensitizers for solar cells.

to massively exploiting fossil fuels as the energy resource. However, the generation speed of fossil fuels is much slower than the depletion rate, leading to human society getting close to an energy and environmental crisis. Solar energy is regarded as one of the perfect energy resources owing to its huge reserves, inexhaustibility and pollution-free character. Directly converting solar light to electric energy based on photovoltaics is the optimal way for electrified modern society. Different technologies in photovoltaics, such as crystalline Si, semiconductor (*e.g.*, GaAs)-based cells, thin-film (*e.g.*, CdTe) solar cells, organic bulk heterojunction (BHJ) solar cells and dye-sensitized solar cells (DSSCs), coexist to compete the future market. Among them, the DSSCs have been considered as a promising generation of photovoltaic techniques due to their unique biomimetic operating principle.¹

The device structure of DSSCs is illustrated in Fig. 1. In brief, such solar cell devices are composed of a transparent conducting oxide (TCO) substrate, a mesoporous semiconductor (predominately TiO_2) film adsorbed with photosensitizer dyes, an electrolyte layer containing a redox couple, and a counter electrode. The photosensitizer dye can absorb sunlight and create a high energy state, from which a photo-excited electron is injected into the conduction band of the TiO_2 semiconductor. After percolation through the thin mesoscopic semiconductor film, the injected electrons are collected by the conducting substrate and flow into the external circuit. Simultaneously, the oxidized sensitizers generated after electron injection are reduced to their neutral state by the reducing species (generally iodide ions) in the electrolyte solution. The oxidized species in the electrolyte diffuse into the counter electrode and receive the external circuit electrons to complete the whole circuit. Such a cycle is kept repeating without any material being consumed but energy being transformed from light to electricity.

Generally, the performances of DSSCs are evaluated by the following parameters: short circuit photocurrent density (J_{sc}),

open circuit photovoltage (V_{oc}), fill factor (FF) and power conversion efficiency (η). Monochromatic incident photon-to-electron conversion efficiency (IPCE) is usually utilized to evaluate the spectral response of solar cells. The definition of these parameters can be found in the previous comprehensive review.² In addition, the lifetime of DSSC devices is critical to the practical applicability. Improving the photovoltaic performances of DSSCs is a systematic engineering, requiring good compatibility among each component in devices. Especially, many researchers put their emphasis on the sensitizer dyes because they play a key role in DSSCs: (i) their absorption properties (including the wavelength range and extinction coefficients) determine the light-harvesting of DSSCs; (ii) their levels of molecular frontier orbitals influence thermodynamics in electron injection and dye regeneration; (iii) their configuration and aggregation state on semiconductor surfaces affect the competition between electron injection and recombination; and (iv) their photo-thermal stability determines the device lifetime to a great extent. The correlation between molecular sensitizer structure and device efficiency is an important issue in DSSC research.³

Presently, organic sensitizers for DSSCs fall into two broad categories: metal-polypyridyl complexes⁴ and pure metal-free organic dyes.² DSSCs based on ruthenium (Ru)-polypyridyl dyes usually show high efficiency (10–11%) due to their wide absorption range from the visible to the near-infrared (NIR) regime, especially being capable of realizing J_{sc} as high as 17–21 mA cm⁻². On the other hand, pure metal-free organic dyes generally possess relatively narrow spectral response (usually in the 400–700 nm range) with lower efficiencies. To date, there are not many pure metal-free organic sensitizers based on the classical iodine electrolyte which are capable of achieving 9% photovoltaic efficiency.² Moreover, achieving the critical device stability is still a great challenge. However, with focus on the cost and limited Ru resource, a metal-free organic sensitizer could become very promising once the efficiency and stability were improved to a viable level. Undoubtedly, molecular engineering is the most effective method to improve the performance from the viewpoint of sensitizers. To date, most of these pure organic sensitizers have been constructed with a typical electron donor- π bridge-electron acceptor (D- π -A) configuration for facilitating photo-induced charge separation.² Some groups even incorporated star-burst multi-donors,⁵ and reconfigured the cross shape of double D- π -A branched dyes,⁶ for modulating the spectral response and energy levels of sensitizers. Several nice reviews have been published to summarize these D- π -A as well as modified organic sensitizers in recent years.^{2,7–11}

Recently, our group has proposed a novel “D-A- π -A” (Fig. 2) concept for designing novel organic sensitizers, in which several kinds of electron-withdrawing units (such as benzothiadiazole, benzotriazole, quinoxaline, phthalimide and diketopyrrolopyrrole) are incorporated into the π bridge to tailor molecular structures and optimize energy levels. We have systematically demonstrated that the incorporated electron-withdrawing additional acceptor can be treated as an “electron trap”, showing several distinguished merits such as: (i) essentially

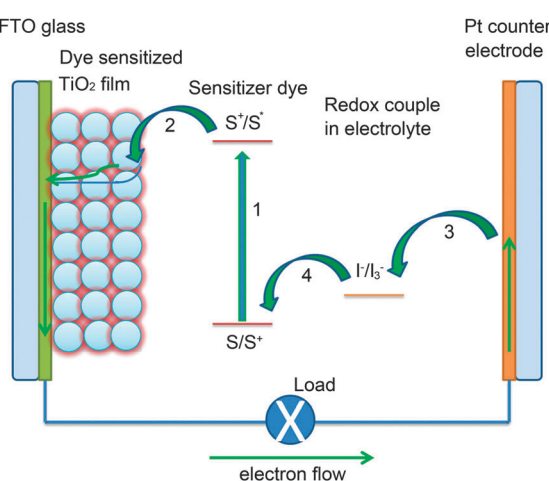


Fig. 1 Schematic diagram of electron transfer processes in DSSCs: (1) photo-excitation, (2) electron injection, (3) redox couple regeneration, and (4) dye regeneration.

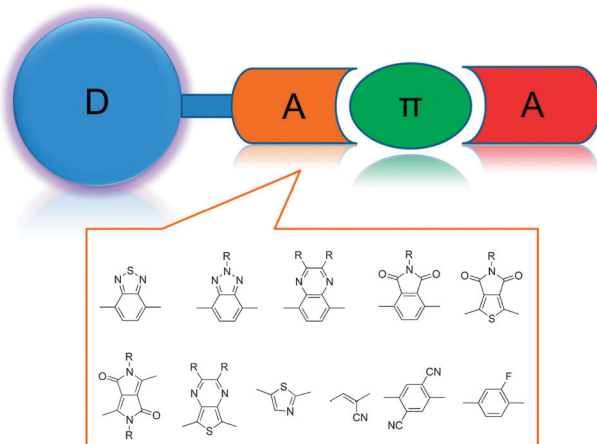


Fig. 2 Configuration of organic D–A– π –A sensitizers as well as building blocks for additional electron-withdrawing acceptors.

facilitating the electron transfer from the donor to the acceptor/anchor; (ii) conveniently tailoring the solar cell performance with a facile structural modification on the additional acceptor; (iii) improving V_{oc} with the nitrogen-containing heterocyclic group; (iv) conveniently tuning the molecular energy gap, and modulating the response of the light-harvesting range with the new resulting absorption band; and (v) most importantly, being capable of greatly improving the sensitizer photo-stability. Here we systematically illustrate the novelty and specificity of D–A– π –A featured sensitizers. Organic sensitizers containing additional electron-withdrawing units (or D–A– π –A dyes) are reviewed with specific concern on the relationship between molecular structures and absorption, energy levels as well as photovoltaic performances.

Benzothiadiazole (BTD) based D–A– π –A featured organic sensitizers

As an important building block, BTD is a strong electron-withdrawing unit with a five-membered heterocyclic ring ($C=N-S-N=C$), exhibiting the electron-deficient character. The four substitution positions on the phenyl ring in BTD provide convenient structure modification. The highest occupied molecular orbital (HOMO) and the lowest unoccupied molecular orbital (LUMO) can be readily tailored with incorporation of BTD in organic materials,^{12,13} inspiring researchers to develop BTD-based organic sensitizers for DSSCs.

Lin *et al.* reported the first BTD-containing organic sensitizers **1** and **2** (Fig. 3) that contain diphenylamine as an electron donor and cyanoacrylic acid as an electron acceptor, bridged with a phenyl or thienyl fused BTD unit.¹⁴ The only structural variation between **1** and **2** is the π -linker between the diphenylamine donor and the BTD unit, which is phenyl for **1** while thienyl for **2**. However, compared to **1**, thienyl-linked **2** shows 0.259 eV up-shift in its HOMO level, and 0.255 eV decrease in the HOMO–LUMO gap, along with a 50 nm bathochromic-shift in the charge-transfer (CT) absorption band. It is worth noting that

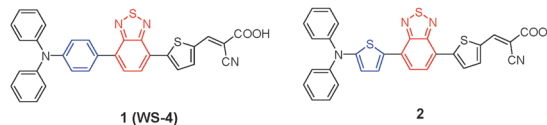


Fig. 3 Chemical structures of BTD-based sensitizers **1** (WS-4) and **2**.

the HOMO levels of sensitizers **1** and **2** are quite sensitive to the donor structure. Sensitizers **1** and **2** show their CT absorption band at 491 and 541 nm, respectively. The underlying reason for the difference in energy levels and absorption spectra between **1** and **2** is that the thienyl segment shows smaller resonance energy and keeps better co-planarity with its neighboring units, which not only provides more effective conjugation but also decreases the energy barrier of charge transfer transition. When sensitizers **1** and **2** were employed in DSSCs, the photovoltaic performance of the latter was unfortunately poorer than the former in spite of their inverse light absorption ranges. Lin *et al.* ascribed the poor performance of **2** to its good molecular co-planarity facilitating the non-radiative decay of excited states with a decrease in the electron injection efficiency.¹⁴ Also, we speculate the possible reasons as follows: (i) the higher HOMO level of **2** possibly leading to insufficient driving force for dye regeneration and (ii) the high co-planarity of **2** leading to unfavorable aggregation on the TiO₂ surface because the authors did not try to exploit co-adsorbents during the device fabrication. Apparently, the molecular structures of BTD-based sensitizers need further optimization if we want to utilize their broad absorption character.

Recently, our group has also introduced the BTD unit into organic sensitizers, and systematically tailored the molecular structures.¹⁵ A series of organic sensitizers **WS-1**–**WS-4** (Fig. 4) was reported, in which the BTD unit was considered as an *additional* electron accepting unit rather than a simple π -bridge building block. Note that **WS-4** is exactly the same as aforementioned **1** in Fig. 3 and just used for parallel comparison. Importantly, a novel concept of the D–A– π –A configuration was proposed to emphasize the effect of the additional electron-withdrawing unit on the conjugated π -spacer. A lot of underlying contributions of the BTD unit (or similar electron-withdrawing units) to organic bipolar sensitizers were explored in depth.

By tuning the electron donor group and π -linker in **WS-1**–**WS-4**, we systematically modulated the molecular HOMO–LUMO energy levels. An indoline derivative as an electron donor in **WS-1** and **WS-2** has been proved to endow stronger electron-donating ability than triphenylamine in **WS-3** and **WS-4**, resulting in a 0.28 eV up-shift in HOMO levels with 36–41 nm red-shift of the CT absorption band. Furthermore, the π -linker between BTD and the cyanoacrylic acid group greatly influences LUMO levels as well as absorption spectra. Compared to the phenyl group, the thienyl linker decreases LUMO energy levels by 0.16 eV (Fig. 4), and extends the CT band to a long wavelength by 37–42 nm. After optimizing the donor and π -linker, **WS-2** shows the smallest molecular HOMO–LUMO energy gap (1.91 eV) and broadest absorption range among

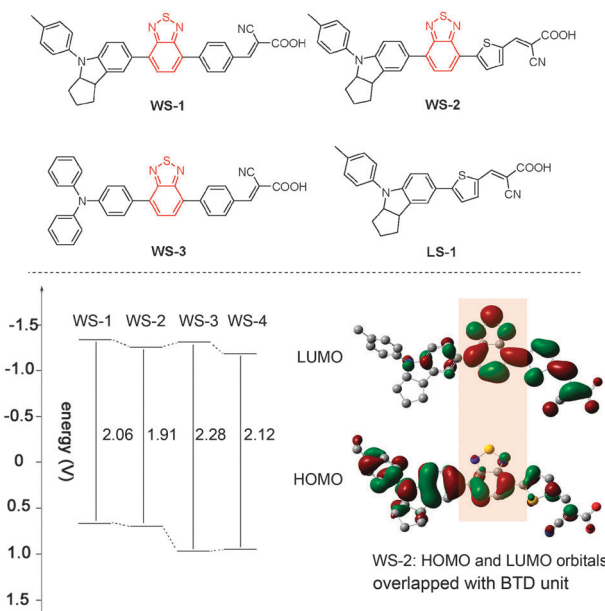


Fig. 4 Top: chemical structures of BTD-based D-A- π -A featured organic sensitizers **WS-1**, **WS-2**, **WS-3**, and reference dye **LS-1**; bottom: HOMO–LUMO energy levels of **WS-1** to **WS-4**; electron distributions of both HOMO and LUMO orbitals for sensitizer **WS-2**.

the four sensitizers. Note that the absorption curve of **WS-2** is very similar to that of **2**. However, **WS-2** based DSSCs show much better photovoltaic performance than **2**, and are the champions among **WS-1**–**WS-4**. Especially, upon co-adsorption with 20 mM deoxycholic acid (DCA) in the dye bath, **WS-2** based DSSCs gave an η of 8.7%. Moreover, this value has been further improved to 9.0% by Grätzel's group in EPFL. Our results overthrow the previous statement that the BTD unit in the π -bridge can hamper the charge transfer from the donor to the anchoring group in a sensitizer molecule and decrease electron injection. In contrast, the density functional theory (DFT) simulation indicates that the distributions of both HOMO and LUMO orbitals for sensitizers **WS-1**–**WS-4** are well overlapped with the BTD unit (Fig. 4), indicating the preferably facilitated electron transition from HOMO to LUMO orbitals. It is convincing that the cascaded electron withdrawal from D to internal A, then to terminal A in the D-A- π -A configuration may benefit charge separation in organic sensitizers.

In the following part, we attempt to interpret contributions of the additional BTD unit to energy level optimization and light harvesting enhancement with sensitizer **WS-2**. To clarify these, a reference D- π -A organic dye **LS-1** (Fig. 4) with very similar structure to **WS-2** but without the BTD unit was introduced for illustration.

Firstly, we can see in Fig. 5 that the presence of a BTD unit in **WS-2** significantly red-shifts its CT absorption band by 48 nm relative to **LS-1**. Moreover, the half-band width of **WS-2** is much larger than that of **LS-1**, resulting in a 100 nm red-shift in absorption threshold, which can greatly enhance the sensitizer light-harvesting in the long wavelength region. Unquestionably, such shifting and broadening of the CT band should be

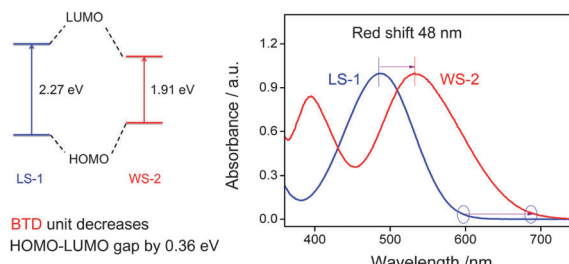


Fig. 5 HOMO–LUMO levels and absorption spectra (in chloroform–methanol mixed solution ($v/v = 4/1$)) of dyes **LS-1** and **WS-2**.

Table 1 Calculated TD-DFT excitation energies (eV, nm), oscillator strengths (f), and composition in terms of molecular orbital contributions of **LS-1** and **WS-2**

Dyes	Bands	Composition ^a	E (eV, nm)	f
LS-1	S1	94% H \rightarrow L	2.57 (481.8)	1.3202
	S2	87% H – 1 \rightarrow L	3.85 (322.4)	0.145
WS-2	S1	77% H \rightarrow L	2.31 (535.9)	1.2417
	S2	34% H \rightarrow L + 1 48% H – 1 \rightarrow L	3.16 (391.8)	0.3657
	S3	28% H – 1 \rightarrow L + 1	4.07 (304.4)	0.1083

^a H = HOMO, L = LUMO, H – 1 = HOMO – 1, L + 1 = LUMO + 1.

attributed to the decreased HOMO–LUMO gap caused by incorporation of BTD (Fig. 5).

Secondly, a new absorption band is observed at around 400 nm for **WS-2** (Fig. 5). To explain the origin of the additional absorption band, the time-dependent density functional theory (TD-DFT) calculation was applied on **WS-2** and **LS-1** (Table 1), indicating that the additional band in **WS-2** corresponds to some secondary frontier orbital transitions, such as from HOMO to LUMO + 1 and from HOMO – 1 to LUMO. In common D- π -A configuration dyes (such as **LS-1**), such secondary transition needs high energy excitation and corresponds to deep UV absorption. However, due to the presence of the BTD unit, the energy for these secondary transitions in **WS-2** decreases dramatically, leading to the absorption band shifting to the visible region. In any way, such a new absorption band improves the light-harvesting of **WS-2** in the short wavelength region.

Thirdly, the electron-withdrawing BTD shows auxiliary function to the anchoring group of carboxylic acid, which is reflected by the dye carboxylic acid deprotonation and/or the chemisorption onto the TiO₂ semiconductor (Fig. 6). **LS-1** exhibits a distinct hypsochromic effect during the adsorption process. It is bright red in solution, while yellow-orange on TiO₂ film. When **LS-1** is anchored onto the nanocrystalline TiO₂ surface, the –COOH group becomes –COOTi, which shows weaker electron-withdrawing ability, leading to a distinct blue-shift of the CT absorption band. Actually, the absorption peak of **LS-1** on 3 μ m TiO₂ film was severely blue-shifted by 66 nm from 486 nm in solution to 420 nm on TiO₂. However, **WS-2** shows an almost negligible hypsochromic shift of the CT band upon adsorption (Fig. 6). The colors of **WS-2** in solution and on TiO₂ are almost the same. We attribute this

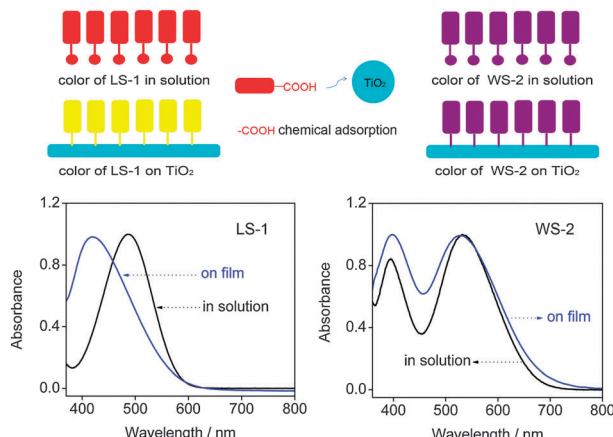


Fig. 6 Top: chemical adsorption of **LS-1** and **WS-2**, showing the auxiliary electron-withdrawing effect of BTD on the terminal acceptor. Bottom: changes in absorption spectra of **LS-1** and **WS-2** in chloroform–methanol mixed solution ($v/v = 4/1$, black line) and on 3 μm TiO_2 film (blue line).

phenomenon to the auxiliary electron-withdrawing effect of BTD on the terminal anchoring acceptor group, that is, the electron-withdrawing character of BTD compensates the weak electron-withdrawing $-\text{COOTi}$. Such a small hypsochromic effect ensures that **WS-2** can maintain high light-harvesting in the long wavelength region on TiO_2 film with a beneficial, broad spectral response.

Finally, the electron-deficient BTD unit can effectively improve the photo-stability of indoline-based organic sensitizers. As electron donors, the indoline derivatives usually show stronger electron-donating ability than traditional triphenylamines.¹⁶ However, the photo-stability of such indoline derivatives is always not good due to their low oxidation potential. Introduction of the BTD unit significantly improves the photo-stability of indoline based compounds. For example, the bromo-substituted indoline (Fig. 7) in CH_2Cl_2 or THF solution is extremely sensitive to light, changing from colorless solution to green and grey in 2–3 hours. In contrast, BTD-indoline becomes very stable, even on keeping for a long time (greater than 2 years). The increase in photo-stability of BTD-indoline is attributed to the beneficial electron distribution between indoline and BTD units. The frontier molecular orbital energies (vs. vacuum) are also listed in Fig. 7. In indoline, both HOMO and LUMO orbitals are

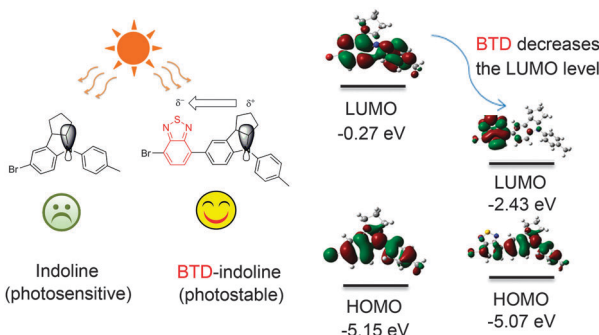


Fig. 7 Mechanism of the BTD unit for increasing the photo-stability of indoline derivatives.

delocalized over the aromatic rings, and the HOMO–LUMO energy gap is as large as 4.88 eV. Therefore, the energy in the excited state of indoline is expected to be very high, and photochemical reactions are possibly allowed to take place, resulting in fast photo-degradation. Differently, in BTD-indoline the LUMO orbital is localized on the BTD unit due to the strong electron-withdrawing nature of the BTD unit. Moreover, the LUMO energy of BTD-indoline is significantly lower than that of bare indoline, resulting in less chemical activity after photoexcitation. Therefore, the photostability is drastically enhanced by the BTD unit.

Besides the photostability, the redox stability is also a key factor for the cell device lifetime because sensitizers are repeatedly oxidized and reduced in working cells. Especially, the oxidized states of sensitizers upon electron injection are most unstable, during which unfavorable photoreactions may occur to wreck the sensitizers and damage the photovoltaic performances. Repeated anodic CV scans on sensitizers in solution can evaluate the redox stability. Obviously, after repeated scans on **WS-2**, its CV curves remain unchanged, suggestive of high redox stability (Fig. 8).

In previous publications, the stability and lifetime of DSSCs based on indoline sensitizers are discussed in short. Some comments^{7,17} show that the long-term stability of traditional indoline-based devices is very poor¹⁸ due to the desorption of dyes from the TiO_2 surface to electrolyte solution. Meanwhile, photo-degradation of indoline-based sensitizers may also lead to the decoloration of devices. However, D-A- π -A featured **WS-2** shows excellent stability both in solution and on TiO_2 film. In addition, **WS-2** based ionic liquid electrolyte DSSCs showed good stability and maintained almost constant high

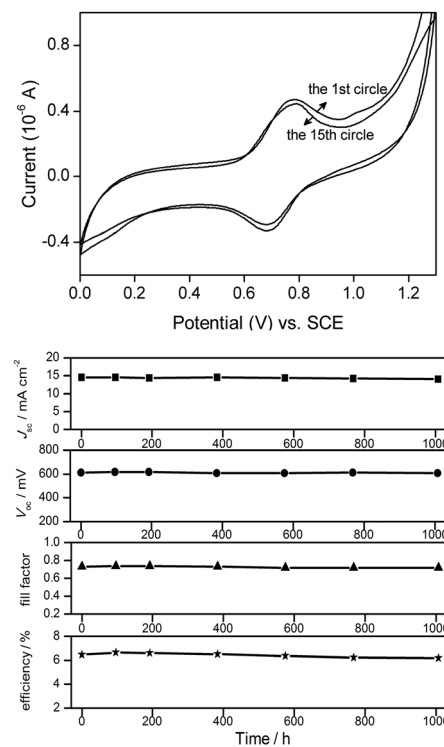


Fig. 8 Top: cyclic voltammogram scan on **WS-2** in CH_2Cl_2 solution; bottom: long term stability of **WS-2** based ionic liquid DSSCs.

performance after 1000 h of light soaking (bottom of Fig. 8).¹⁵ This is the first stability test for DSSCs based on indoline sensitizers, indicating that the low stability of indoline-based organic sensitizers can be distinctly improved by such D-A- π -A configurations.

Here, we demonstrate the contribution of the BTD based D-A- π -A configuration to the energy level optimization and light harvesting enhancement (red-shift of the CT band, generation of additional absorption bands, decrease of the hypsochromic effect on TiO₂ film, and improvement of the stability of indoline-based organic sensitizers), especially with respect to the common D- π -A configuration. Actually, the similar D-A- π -A featured sensitizers with other kinds of electron-withdrawing building blocks (such as quinoxaline, DPP, etc.) also show these similar merits to a different extent, which will be manifested in the subsequent discussions.

The high performance of WS-2-based DSSCs should be ascribed to its wide spectral response and high photocurrent. However, the V_{oc} values of WS-2-based DSSCs are relatively unsatisfactory (usually 600–650 mV). Hence, we further designed another sensitizer WS-6 (Fig. 9) by adopting an *n*-hexyl alkyl chain substituted thiienyl unit instead of the bare thiienyl in WS-2.¹⁹ Since the *n*-hexyl chain in WS-6 does not affect its electronic conjugation, the two dyes show almost the same molecular energy levels and absorption spectra in solutions. However, the alkyl chain plays an important role when sensitizers are adsorbed onto the TiO₂ surface, which can reduce intermolecular aggregation, and improve electron injection efficiency.²⁰ Aggregation may lead to intermolecular quenching or molecules residing in the system not functionally attached to the TiO₂ surface and thus acting as filters, which will decrease the electron injection greatly.¹⁰ Moreover, the hydrophobic alkyl chains between TiO₂ and electrolyte can suppress dark current.²¹ It is believed that the grafted chains can facilitate the formation of a compact dye layer, which blocks the dark current from TiO₂ to the electrolyte.²² Either the hydrophobic character or the compact dye layer is beneficial for improving V_{oc} of DSSCs. Under the same conditions for device fabrication (without DCA co-adsorption, Fig. 9), sensitizer WS-6 gave a higher V_{oc} (672 mV) than WS-2 (600 mV). Electrochemical impedance spectroscopy (EIS) measurements indicate that the resistance for charge recombination (from TiO₂ to the electrolyte under open-circuit conditions) in WS-6 based DSSCs is much larger than that of WS-2. Hence the loss of injected electrons is decreased in WS-6, resulting in higher electron density in the TiO₂ conduction band with a higher V_{oc} output. Obviously, the introduction of alkyl chains is effective in improving open-circuit voltage and power conversion efficiency. However, compared with the high stability of WS-2, we found that the photo-stability of WS-6 sensitized TiO₂ film was decreased to some extent. The degradation of WS-6 on TiO₂ film might arise from the oxidation of the *n*-hexyl chain on the thiienyl unit.²³

Dithienyl-fused BTD (Fig. 10) is a common building block for constructing BTD based oligomers or polymers.^{24–26} The thiienyl units keep good co-planarity with the BTD core, thus obtaining broader absorption *via* simple structure modification.

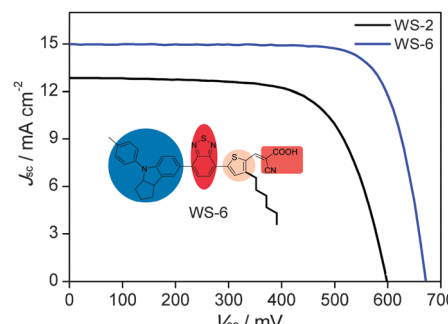


Fig. 9 J-V curves for WS-2 and WS-6 under the same conditions (without co-adsorbent). Inset: chemical structure of WS-6.

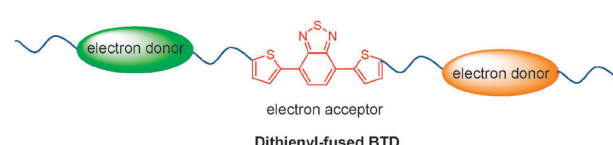


Fig. 10 Oligomers or polymers with dithienyl-fused BTD as an electron acceptor.

To date, several groups have adopted dithienyl-fused BTD for constructing efficient organic molecular sensitizers. Kim *et al.* utilized dithienyl-fused BTD to construct D-A- π -A sensitizers 3–6 (Fig. 11) with different linking groups (single, double and triple bonds) between the triphenylamine donor and the BTD segment.²⁷ Compared to the single bond in 3 ($\lambda_{max} = 533$ nm in CH₂Cl₂), the double bond (4) can red-shift the CT band by 13 nm, while the triple bond (5) blue-shifts the CT band by 18 nm. On the other hand, the peripheral alkoxy groups on the triphenylamine unit (6) also result in 9 nm red-shift of the CT band with respect to 3. Clearly, the double bond and alkoxy groups can broaden the light-harvesting of sensitizers to some extent. However, their effects on photovoltaic performances are different. In DSSCs, sensitizer 4 containing a double bond shows much lower performance than 6, and even worse than 3 and 5. With the almost same absorption range, DSSCs based on sensitizer 4 only showed a J_{sc} of 10.6 mA cm⁻², while 6 gave a high J_{sc} of 17.9 mA cm⁻² and an η of 7.3%. It seems that double and triple bonds are not suitable to connect the electron donor and dithienyl-fused BTD for highly efficient organic sensitizers. Note that the high performance of sensitizer 6 is critically dependent upon DCA co-adsorption.

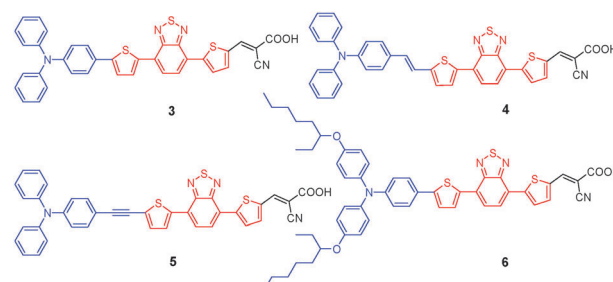


Fig. 11 Chemical structures of dithienyl-fused BTD based sensitizers 3–6.

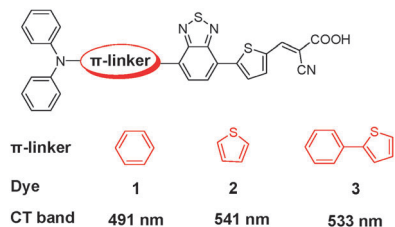


Fig. 12 Effect of the π -linker between diphenylamine and BTD on absorption bands.

It is indicated that dithienyl-fused BTD constructed organic sensitizers easily aggregate on TiO_2 films due to their good planarity. Even sensitizer **6** containing a couple of long and branched alkoxy chains still needs a large amount of co-adsorbent. From another point of view, the introduction of alkyl chains on a donor part may have a little effect in preventing the molecular π -aggregation, and the most effective way to prevent π -aggregation is still the incorporation of long alkyl chains grafted onto the planar π -linker segment.²⁸

Here, an interesting comparison could be carried out between sensitizers **1**, **2** and **3** (Fig. 12). All the three dyes have the same structure except the different π -linker between diphenylamine and BTD. Their CT bands in THF solution are in the order of **1** (491 nm) < **3** (533 nm) < **2** (541 nm), with a reversal sequence of the HOMO-LUMO gap. Sensitizer **3** with a longer π -conjugation length (combination of phenyl and thiényl units) shows a shorter CT absorption band than **2**, hinting that the elongation of the π -bridge is not always effective in red-shifting absorption spectra. In addition, the linking manner between the electron donor and acceptor is important. As a common π -linker, the thiényl unit is beneficial to conjugation because of high polarizability and small steric hindrance with its neighboring units. In contrast, the phenyl group usually shows a large twist with neighboring units in the π -bridge, which is unfavorable for effective conjugation. Generally, it is difficult to obtain long wavelength absorption from multi-phenyl linked organic sensitizers.

In Fig. 13, these sensitizers are also designed with a dithienyl-fused BTD as the core. The aggregation problem is considered from different aspects. Ko *et al.* reported the dithienyl-fused BTD based organic sensitizers **7** and **8**, using a bis-dimethylfluorenylamino moiety as the electron donor.²⁹ Several contributions have been focused on the fluorenyl unit as the π -linker of organic sensitizers due to its rigid planar structure. However, fluorenyl bridged sensitizers often show narrow absorption spectra because they usually form a large torsion with their neighboring groups.³⁰ The fluorenyl-featured electron donor in **7** and **8** is expected to enhance the electron-donating capability, and hinder the unfavorable aggregation on TiO_2 film. However, compared to dye **3**, the dimethylfluorenylamino donor in **7** shows little preferable effect on the CT absorption band (both in THF, 533 nm for **3**; 534 nm for **7**), demonstrating that the electron-donating capability of the fluorenyl-featured donor is not enhanced with respect to the classical triphenylamine group. It is quite interesting that sensitizer **8** shows distinct narrower

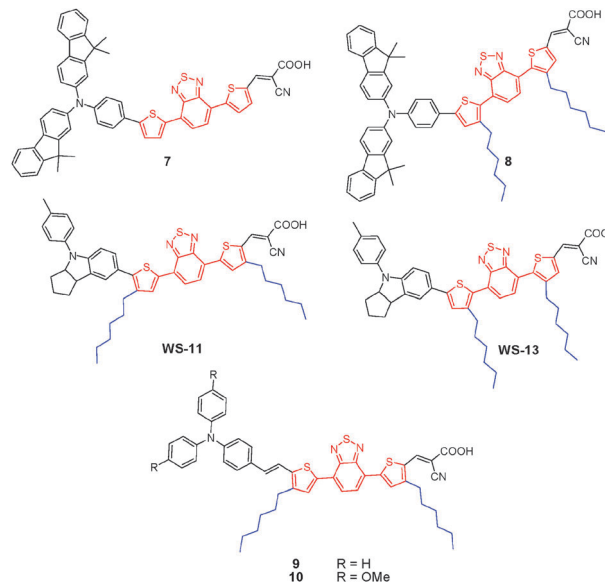


Fig. 13 Chemical structures of dithienyl-fused BTD based sensitizers **7**, **8**, **9**, **10**, WS-11 and WS-13.

absorption spectra than **7** only due to the introduction of a pair of *n*-hexyl chains onto thiényl units. The presence of these *n*-hexyl chains causes a large blue-shift by 66 nm in the CT absorption band. DFT simulation indicates that the alkyl chain can cause augmentation of steric hindrance, resulting in a severely twisted configuration and less conjugation degree. The dihedral angle between BTD and the thiényl unit is 5.8° and 44.4° for **7** and **8**, respectively. Apparently, the introduced alkyl chains and twisted configuration in **8** are unfavorable for light-harvesting, but extremely benefit from suppressing π - π stacking. In DSSCs, the J_{sc} of sensitizer **8** is not very high due to its limitation in spectral response. However, sensitizer **8** based devices show better photovoltaic performances (mainly higher V_{oc}) than **7**. To obtain higher performance, the spectral response and configuration control should be well balanced on sensitizers.

In our group, two dithienyl-fused BTD based organic dyes WS-11¹⁹ and WS-13 (Fig. 13) with an indoline unit as an electron donor group were developed for obtaining further insight into the alkyl chain effect on CT absorption. Compared with WS-6, the grafted *n*-hexylthiophene in WS-11 extends the photoresponse to a panchromatic spectrum with a CT band at 557 nm in CH_2Cl_2 . However, the CT band of WS-13 is blue-shifted, and located only at 505 nm with a distinct increase in the HOMO-LUMO gap only due to the different positions of alkyl chains. Accordingly, we consider that the substitution position of alkyl chains on the thiényl unit has a crucial influence on the molecular electronic structure as well as absorption property. We might draw a relationship with alkyl chains as follows:

Case 1: if the alkyl chains are attached on the thiényl *meta*-position away from the BTD unit (WS-11), the good delocalization and conjugation across the BTD and thiényl units can be maintained, usually along with a CT absorption band similar to

that without alkyl chains (7). Case 2: if the alkyl chains are fixed on the thiienyl *ortho*-position near the BTD unit (**8** and **WS-13**), the steric effect of alkyl chains in small space makes the thiienyl unit twist, resulting in relatively large dihedral angles to block the conjugation with a severe blue-shift of the CT band. Moreover, the steric effect of alkyl chains not only exists in the BTD system, but also can cause molecular configuration twist even in the oligothiophene system.³¹ Accordingly, although the introduction of alkyl chains into organic sensitizers can suppress the aggregation and reduce the charge recombination in DSSCs, the substitution position for introduced alkyl chains should be carefully taken into account. Its effect on molecular electronic structure and absorption (relative to the light-harvesting) could not be overlooked. Notably, **8** and **WS-13** are some of the few BTD based organic sensitizers, which can attain V_{oc} higher than 700 mV (Table 2). However, such a high V_{oc} is sacrificed with the loss of spectral response and photocurrent, which principally limits the potential of further promoting the power conversion efficiency of DSSCs.

Pei *et al.* reported the dithienyl-fused BTD based dyes **9** and **10** (Fig. 13).³² Their alkyl chains are away from the BTD core, and their absorption properties are consistent with our aforementioned alkyl chain effect. The methoxy groups in **10** shift the CT band to the long wavelength region by 17 nm relative to **9**. In DSSCs, sensitizer **9** shows larger J_{sc} (16.46 mA cm⁻²) and higher power conversion efficiency (6.04%) than that of dye **10** (11.94 mA cm⁻², 4.68%). The authors explained that the driving force for dye regeneration and electron injection in **10** is insufficient. In other words, the modulation of the molecular energy gap in dye **10** is overdone to some extent. Additionally, the CT band of **9** shows a red-shift by 11 nm with respect to dye **4** (Table 2), revealing that the alkyl chains in **9** seem beneficial

to the molecular co-planarity, along with little steric-hindrance to BTD. Moreover, the performance of **9** in DSSCs is much better than **4**, hinting that the real reason for low η of **4** is not the mismatch in energy levels but strong aggregation. Again, a suitable substitution position for alkyl chains can play a great role in both absorption and self-anti-aggregation ability.

The former discussions are focused on the electron donor, π -bridge and alkyl chain in BTD-based organic sensitizers. In the following part, we discuss the linker effect between the anchoring group and BTD unit. As shown in Fig. 14, the anchoring group of cyanoacrylic acid is directly or indirectly linked to the BTD core. Park *et al.* reported BTD-based sensitizers **11** and **12**.³³ In **11**, the anchoring group of cyanoacrylic acid is directly connected to the BTD core, while in **12**, the BTD and cyanoacrylic acid are separated by a phenylenevinylene, which increases the distance and conjugation between BTD and the anchoring group. Intriguingly, the π -extension by phenylenevinylene does not lead to any red-shift of the CT band (498 and 494 nm for **11** and **12**, respectively). Cyclic voltammograms indicate that the HOMO–LUMO levels of both dyes are very similar in solution. When employed in DSSCs, **12** shows much better performance than **11**. The authors used nanosecond transient absorption spectroscopy to investigate the difference in electron injection efficiency between the two dyes. They monitored the recovery of the dye ground state after a pulse of photo-excitation on a dye-loaded TiO₂ film. As found, the regeneration of **11** is much faster than **12**, indicating that the recombination of injected electrons with oxidized dyes in **11** is worse than that of **12**.

Coincidentally, Bäuerle *et al.* also investigated the interesting phenomenon mentioned above.³⁴ They designed BTD-based organic dyes **13** and **14** (Fig. 14). Similar to dye **11**, the electron acceptor (cyanoacrylic acid) of dye **13** is directly connected to BTD. The difference is that the insertion of a phenyl unit in **14** between the BTD and cyanoacrylic acid causes a large blue-shift by 55 nm in the CT absorption band with respect to dye **13**. Such a blue-shift is not observed in dye **12**, implying that the phenyl linker can interrupt molecular conjugation to some extent. Similarly, dye **14** shows much better performance than **13** in DSSCs. To explain this phenomenon, a series of experiments on the two dyes were carried out, including

Table 2 Photophysical and photovoltaic performances of DSSCs based on BTD-containing D–A– π –A featured organic sensitizers

Dye	CT band/nm	E_{0-0}/eV	$J_{sc}/\text{mA cm}^{-2}$	V_{oc}/mV	FF	$\eta/\%$	Ref.
1	491 ^a	2.121	10.44	546	0.66	3.77	14
2	541 ^a	1.866	3.21	517	0.69	1.15	14
WS-1	496 ^b	2.06	11.9	650	0.68	5.3	15
WS-2	533 ^b	1.90	17.7	650	0.76	8.7	15
WS-3	455 ^b	2.27	9.5	690	0.75	4.9	15
WS-4	497 ^b	2.11	11.2	600	0.75	5.0	15
WS-6	547 ^c	2.06	15.00	672	0.77	7.76	19
3	533 ^a	1.97	15.0	580	0.65	5.72	27
4	546 ^a	1.93	10.6	540	0.59	3.37	27
5	515 ^a	2.11	13.0	560	0.63	4.55	27
6	542 ^a	1.93	17.9	620	0.66	7.30	27
7	534 ^d	1.93	17.10	610	0.72	7.51	29
8	468 ^d	2.07	14.98	770	0.77	8.19	29
WS-11	557 ^c	1.85	10.4	629	0.71	4.64	19
WS-13	505 ^c	2.15	12.20	705	0.75	6.45	
9	557 ^a	1.86	16.46	545	0.67	6.04	32
10	574 ^a	1.55	11.94	555	0.71	4.68	32
11	498 ^d	1.92	8.13	470	0.651	2.49	33
12	494 ^d	1.85	12.24	549	0.566	3.80	33
13	570 ^c	1.67	6.04	423	0.70	1.78	34
14	515 ^c	1.98	18.47	640	0.69	8.21	34
WS-9	536 ^c	2.05	18.00	696	0.72	9.04	35

^a In THF. ^b In CHCl₃ + MeOH. ^c In CH₂Cl₂. ^d In C₂H₅OH.

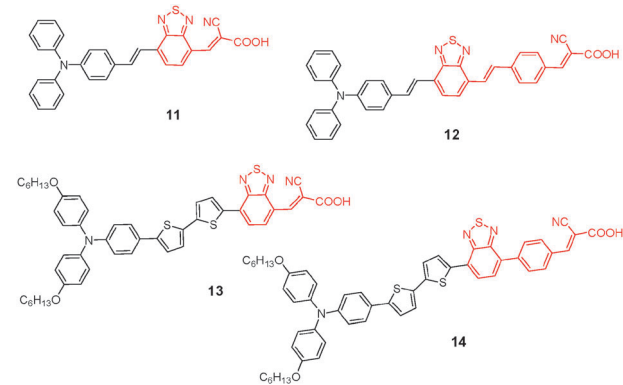


Fig. 14 Chemical structures of sensitizers **11**, **12**, **13** and **14**.

transient photovoltage/photocurrent measurements, time-correlated single photon counting technique, nanosecond laser photolysis, ultrafast transient absorption and electrochemical impedance spectroscopy. As found, solar cells with dye **13** exhibit ample injection efficiencies, but suffer from unusually fast recombination with injected electrons in TiO_2 . Due to the electron-deficient character of BTD, the electron recombination between TiO_2 and oxide dyes under open-circuit conditions is crucial. Based on four dyes in Fig. 14, we take into account the molecular structure in designing the anchoring part in BTD based organic dyes, that is, the additional electron acceptor of the BTD unit should be placed away from the anchoring group by a rigid linker to block the electron recombination between TiO_2 and dye cations. The ingenious molecular design and meticulous research on dyes **13** and **14** give a very deep insight into the modulation of molecular structures. Nevertheless, we consider that the phenyl π -linker between BTD and cyanoacrylic acid seems still not suitable because it leads to severe blue-shift in absorption and limits the light-harvesting range. The alternative to this π -linker can be a thiophenyl or multi-thiophenyl unit, which can not only guarantee a good electronic conjugation, but also assure enough distance to avoid charge recombination between TiO_2 conduction band electrons and the oxidized dyes.¹⁰

In our recent work, we have employed a bithiophene as the π -bridge to link the BTD and anchoring group to develop dye **WS-9** (Fig. 15a).³⁵ The bithiophene linker is better than the phenyl linker in sensitizer **14** since it not only puts the BTD unit away from the anchoring group, but also keeps a good conjugation across the whole molecule. Compared with previous

WS-2 and **WS-6**, the extension of the π -bridge in **WS-9** shows a little effect on the CT band. **WS-2** and **WS-9** were carefully studied with focus on absorption and energy levels. In DSSCs, performances of **WS-2** are strongly dependent upon the adsorption conditions (dye bath solvent and co-adsorbent, Fig. 15b). **WS-9** based DSSCs showed comparable photocurrent, but much higher photovoltage (around 100 mV) than dye **WS-2** under the same conditions. After optimization, **WS-9** based DSSCs resulted in high power conversion efficiency (>9%), realizing a breakthrough for BTD-based organic sensitizers.³⁵

Besides the high efficiency, we have carefully investigated the photo-stability of sensitizers **WS-2**, **WS-9** and **LS-1**. Katoh *et al.* developed a simple and efficient method to evaluate the stability of sensitizers.³⁶ Since the most unstable state of sensitizers is their oxidized state, the corresponding sensitizers must remain stable in the cation state for at least 10 s to be capable of realizing a 10-year operation cycle. Actually, we can accelerate the dye aging process upon light irradiation on dye-loaded TiO_2 film without a redox electrolyte (Fig. 15c) because the dye regeneration process under this condition occurs in the millisecond time range, thus taking 10^4 to 10^3 times longer than that in a complete solar cell device (100 ns–1 ms).³⁶ In short, we can measure the absorption spectra of dye-loaded TiO_2 film before and after AM 1.5 simulated solar light irradiation, and observe the variation in the absorption curves upon irradiation. The less decrease in absorbance means the higher photo-stability to corresponding sensitizers (Fig. 15d). Fig. 15e shows the photograph of **WS-2**, **WS-9** and **LS-1** loaded TiO_2 films after AM 1.5 light irradiation for 30 min. Obviously, the photo-stability of BTD-containing **WS-2** and **WS-9** is much higher than that of **LS-1** (Fig. 15f–h). Moreover, the photo-stability of **WS-2** seems a little higher than that of **WS-9**, implying that the incorporation of the hexyl chain on the thiophene bridge in **WS-9** might decrease its intrinsic photo-stability to some extent.^{23,37}

As listed in Table 2, several reported BTD-based D-A- π -A featured organic sensitizers have already shown very promising photovoltaic performance ($\eta > 8\%$) at the present device fabrication level. It is definitely possible for these BTD-based sensitizers to obtain higher efficiency if advanced technologies (including semiconductor film morphology, a new redox couple for the electrolyte and counter electrode) are applied. Generally in BTD-based D-A- π -A featured sensitizers, the BTD unit is introduced for the purpose of decreasing the molecular HOMO-LUMO energy gap, thus extending the absorption range and attaining high photocurrent. Among the reported BTD-based D-A- π -A featured sensitizers, **WS-2**, **6**, **7**, **14** and **WS-9** show high photocurrent ($J_{sc} > 17 \text{ mA cm}^{-2}$ under AM 1.5 and 100 mW cm^{-2} , comparable to N719), suggesting that the extension of the spectral response can be easily achieved in BTD-based D-A- π -A organic sensitizers by the proper molecular engineering. The reason that the other dyes give relatively low J_{sc} might arise from the following facts: (i) insufficient absorption range ($\lambda_{max} < 530 \text{ nm}$ in DCM, THF or commonly used organic solvents) caused by the twisted molecular configuration with disturbed conjugation; (ii) insufficient driving force for

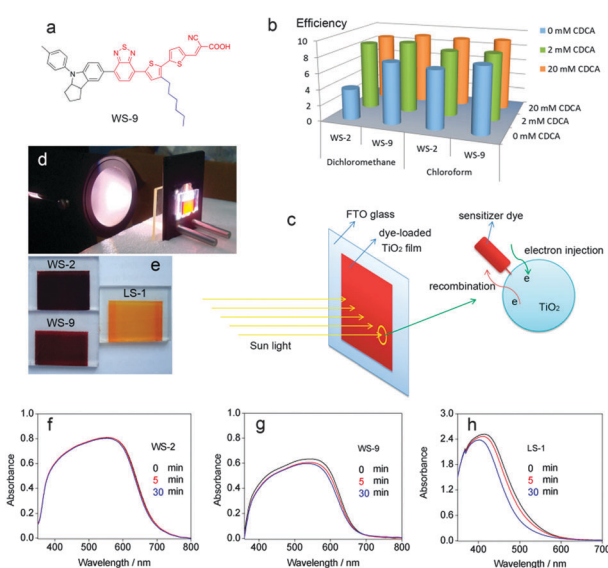


Fig. 15 (a) Chemical structure of sensitizer **WS-9**; (b) effect of dye bath solvent and co-adsorbent CDCA on photovoltaic performances of **WS-2** and **WS-9**; (c) light irradiation on dye-loaded TiO_2 film; (d) photo-stability measurement of sensitizer dyes on TiO_2 film; (e) photograph of dyes **WS-2**, **WS-9** and **LS-1** on TiO_2 films; (f–h) variation in absorbance of **WS-2**, **WS-9** and **LS-1** on TiO_2 films ($6.0 \mu\text{m}$) before and after 5 and 30 min AM 1.5 irradiation (black line: before irradiation; red line: 5 min of irradiation; blue line: 30 min of irradiation).

electron injection and/or dye regeneration resulted from the over-adjusted HOMO-LUMO energy gap, and (iii) an unbeneficial linking group like a double or triple bond inducing the quenching of excited states. Accordingly, more attention should be paid to the screening of donor and linker groups for further developing BTD-based sensitizers. In addition, the relatively low V_{oc} may be the main drawback upon the introduction of the BTD unit into the common D- π -A organic sensitizers. Most DSSCs based on D-A- π -A featured BTD dyes show $V_{oc} < 650$ mV under AM 1.5 and 100 mW cm⁻². The experience of **WS-9** may provide efficient guidance on further molecular structure tailoring for overcoming the V_{oc} limitation.

Benzotriazole, quinoxaline and phthalimide based D-A- π -A featured organic sensitizers

Benzotriazole, as a very cheap and commercially available chemical material, has been broadly utilized in electroplating the surface of purified silver, copper and zinc. In recent years, benzotriazole based π -conjugated polymers have also been explored in photovoltaic cells because of their chemical and environmental stability as well as their electronic tenability.^{38,39} However, the utilization of the benzotriazole unit in molecular sensitizers for DSSCs is seldom reported. Recently, our group has incorporated the benzotriazole unit into indoline and triphenylamine based organic dyes to develop D-A- π -A featured organic sensitizers (**WS-5** and **WS-8**, Fig. 16).⁴⁰ Compared to the BTD unit, the sulfur atom is replaced by nitrogen in the benzotriazole unit.

The incorporation of the benzotriazole unit in **WS-5** and **WS-8** was based on the following considerations: (i) similar to BTD, the electron-withdrawing property of benzotriazole can decrease the molecular HOMO-LUMO energy gap; (ii) the benzotriazole unit provides a facile structural modification on the nitrogen site; (iii) the benzotriazole unit may benefit from reducing charge recombination due to the absence of the sulfur atom;^{41,42} and (iv) the nitrogen-based heterocyclic group of benzotriazole may lift the conduction band edge of TiO₂ and

improve V_{oc} . Actually, many nitrogen-based heterocyclic derivatives including imidazole, triazole, pyrimidine and benzimidazole have been tested as additives in the electrolyte for the sake of increasing V_{oc} . Generally, the V_{oc} enhancing properties of nitrogen-based heterocycles are attributed to binding to the TiO₂ surface or possible binding protons to moderate pH. We attempt to specify whether the nitrogen-based heterocycle is effective when involved in sensitizers. Considering that the heterocycles in sensitizers are spatially away from the TiO₂ surface, we found that the nitrogen-based heterocycles in sensitizers are more prone to bind protons to moderate the pH, not to the TiO₂ surface. In addition, compared with benzothiadiazole-based sensitizers, the benzotriazole unit contains no sulfur element which is attractive to iodine in the electrolyte. Therefore, the benzotriazole-based sensitizers are expected to decrease the iodine concentration at the vicinity of TiO₂ and reduce charge recombination, which is a main reason for low V_{oc} of iodine system based DSSCs.

WS-5 and **WS-8** only differ in the alkyl chain length on the benzotriazole unit; hence the absorption spectra of both dyes are very similar with a strong CT band at around 500 nm in CH₂Cl₂. When applied in co-adsorbent free DSSCs, **WS-2**, **WS-8** and **WS-5** show V_{oc} of 600, 680 and 780 mV, respectively. **WS-8** shows an increment in V_{oc} by 80 mV with respect to **WS-2**, indicating that the benzotriazole unit is indeed effective in increasing V_{oc} . Moreover, the significant enhancement of V_{oc} from methyl (**WS-8**, 680 mV) to octyl (**WS-5**, 780 mV) based sensitizers is attributed to the suppressed charge recombination. Although many works have already certified that introduction of long alkyl chains into dye sensitizers is beneficial for improving V_{oc} and power conversion efficiencies, however, those alkyl chains are substituted on thiophene units, which can easily induce photon-degradation and is harmful to dye stability.^{23,35} Here, the attachment of the octyl group on the nitrogen atom in the benzotriazole unit offers an alternative choice to improve the sensitizer photostability as well as the high anti-aggregation effect.

Another series of D-A- π -A benzotriazole-based organic dyes **15–18** were designed with triphenylamine as the electron donor unit to systematically compare the influence of alkyl substituents (linear or branched alkyl chains) and π -linkage (thienyl or furyl) on photovoltaic performances.⁴³ The chemical structure of **15** is pretty similar to that of **WS-5** except for the donor moiety. The CT absorption band is red-shifted by 38 nm from **15** to **WS-5**, which is in agreement with the experience in BTD-based dyes (such as dyes **WS-2** and **WS-4**).¹⁵ These triphenylamine-based benzotriazole dyes show a very similar CT band at around 450 nm. When employed in DSSCs, both the branched alkyl chain and the furan unit are beneficial for improving V_{oc} . Therefore, **18** gave the highest V_{oc} of 834 mV among four dyes (**15**, **16**, **17** and **18**). Compared to the linear alkyl chain, the branched alkyl chain is considered to cause more steric hindrance, which is favorable for suppressing dye aggregation and retarding charge recombination in DSSCs.⁴⁴ The contribution of the furan linker to V_{oc} may arise from the relatively low affinity between the oxygen and iodide, which potentially decreases the iodide concentration near the TiO₂ surface.⁴¹

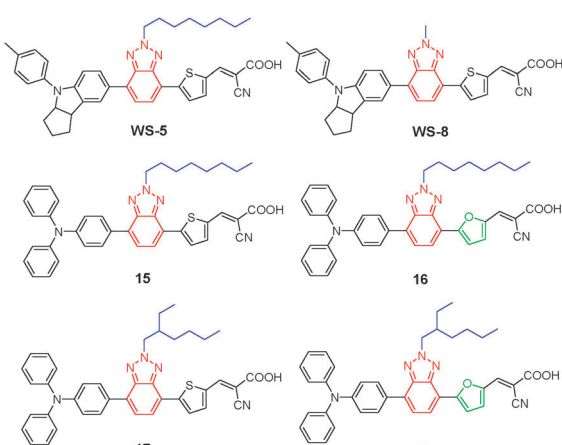


Fig. 16 Chemical structures of benzotriazole-based D-A- π -A sensitizers.

The excellent photovoltaic performances (especially high V_{oc}) of these benzotriazole-based organic dyes demonstrate that incorporation of the benzotriazole unit into the dye skeleton is a promising approach to develop high efficiency organic sensitizers. The main problem of benzotriazole-based organic dyes is their relatively narrow absorption range. As listed in Table 3, the E_{0-0} data of these sensitizers are often greater than 2.0 eV, and the CT bands are all below 500 nm. It might be shown that the electron-withdrawing capability of the benzotriazole unit is not as strong as that of the above-mentioned BTD counterpart. The insufficient light-harvesting range limits the photocurrent improvement in spite of their high V_{oc} . However, the suitable molecular engineering may efficiently extend the absorption band in benzotriazole-based organic sensitizers.

So far, the broad spectral response with high photocurrent has been easily achieved in BTD-based sensitizers, while their V_{oc} is always limited to 700 mV; in contrast, the high V_{oc} is easy to realize in benzotriazole-based sensitizers but their photocurrent becomes discouraging to some extent. It would be desirable to possess both the high J_{sc} of BTD-dyes and high V_{oc} of benzotriazole-dyes simultaneously. Further molecular engineering should turn to this wonderful direction. In other words, the additional electron-withdrawing unit in the D-A- π -A configuration should be carefully screened to well control its absorption band gap by optimizing the interfacial environment in DSSCs. Given that the electron-withdrawing ability of BTD is somewhat too strong while that of benzotriazole is a little weak, moderate options are concentrated on benzoheterocycles such as benzothiazole, benzimidazole and quinoxaline. As illustrated below, the quinoxaline is found to be an ideal electron-withdrawing unit for constructing efficient D-A- π -A featured sensitizers, which exactly combines the merits of both BTD and benzotriazole, especially promising photocurrent and photovoltage.

It is well-known that quinoxaline is a strong electron-withdrawing unit due to its high electron affinity arising from the two symmetric unsaturated nitrogen atoms. Actually, the

Table 3 Photophysical and photovoltaic performances of DSSCs based on benzotriazole-, quinoxaline- and phthalimide-containing D-A- π -A featured organic sensitizers

Dye	CT band/nm	E_{0-0}/eV	$J_{sc}/\text{mA cm}^{-2}$	V_{oc}/mV	FF	$\eta/\%$	Ref.
WS-5	496 ^a	2.12	13.18	780	0.78	8.02	40
WS-8	495 ^a	2.09	13.39	680	0.74	6.74	40
15	454 ^a	1.89	13.26	804	0.66	7.02	43
16	458 ^a	2.12	12.58	824	0.66	6.85	43
17	449 ^a	2.03	13.36	806	0.66	7.05	43
18	450 ^a	2.07	12.64	834	0.64	6.72	43
19	495 ^c	2.18	11.4	660	0.74	5.56	45
20	390 ^b	2.57	6.4	720	0.71	3.30	45
IQ1	521 ^a	1.98	13.60	685	0.67	6.24	46
IQ2	523 ^a	1.97	15.65	776	0.70	8.50	46
TQ1	469 ^a	2.16	10.83	675	0.71	5.19	46
TQ2	470 ^a	2.18	13.51	749	0.70	7.08	46
LS-2	442 ^a	2.30	10.06	748	0.68	5.11	49
21	485 ^c	2.04	13.18	550	0.65	4.71	50
22	510 ^c	1.97	8.90	430	0.65	2.49	50

^a In CH_2Cl_2 . ^b In CHCl_3 . ^c In THF.

quinoxaline unit becomes an attractive component for constructing novel D-A- π -A organic sensitizers due to its diverse structural modifications and intrinsic strong electron-withdrawing properties. Park *et al.* reported quinoxaline-based dyes **19** and **20** (Fig. 17).⁴⁵ At the same time, our group also developed a series of quinoxaline dyes **IQ1**, **IQ2**, **TQ1** and **TQ2** (Fig. 17).⁴⁶ Dyes **19** and **20** were designed with horizontal and vertical electron flow through the quinoxaline core. The absorption spectrum of dye **19** is much broader than that of **20**, hinting that the charge transfer process is more effective in the horizontal case. The photovoltaic performances of the two dyes also prove that the horizontal design is more reasonable. As discussed above, the alkene group in dye **19** between triphenylamine and quinoxaline is not beneficial to the DSSC performance and stability. In our system, the donor part is directly connected to the quinoxaline unit. The CT bands of these quinoxaline dyes are in the sequence of **20** < **TQ dyes** < **19** < **IQ dyes**. When used in DSSCs, the indoline-containing dyes **IQ1** and **IQ2** show higher J_{sc} than the triphenylamine ones due to the extended photocurrent response range. **IQ2** and **TQ2** with long octyl chains show much higher V_{oc} than **IQ1** and **TQ1** with short methoxy groups. Experiments verify that the long alkyl chains in **IQ2** are effective in suppressing dye aggregation on TiO_2 film, and the co-adsorption with CDCA can decrease the photovoltaic performance by decreasing J_{sc} . As a coadsorbent-free sensitizer, **IQ2** combines high J_{sc} and V_{oc} , resulting in a power conversion efficiency of greater than 8.5% under standard measurement conditions.⁴⁶ Also, the photo- and thermal-stability of **IQ2** is pretty good, and ionic liquid electrolyte based solar cells show constant performance during 1000 h of light soaking.

Quinoxaline-based D-A- π -A organic sensitizers also exhibit three absorption bands. The contribution of each absorption band to intramolecular charge separation and photo-induced electron injection is carefully studied by TD-DFT calculation.

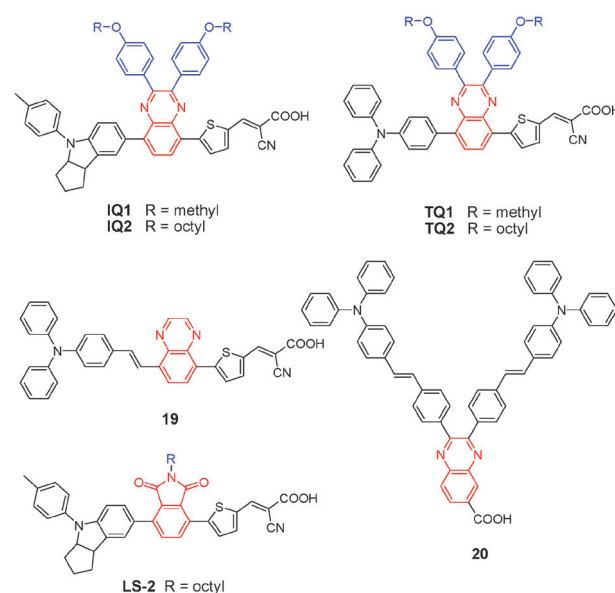


Fig. 17 Chemical structures of quinoxaline and phthalimide-based D-A- π -A organic sensitizers.

For instance, **IQ1** shows three absorption bands at 521 (band I), 406 (band II) and 328 nm (band III, Fig. 18).⁴⁶ TD-DFT simulation indicates that the band I corresponds to HOMO \rightarrow LUMO electron transition; band II is caused by HOMO - 1 \rightarrow LUMO and HOMO - 2 \rightarrow LUMO transitions; band III is due to HOMO - 1 \rightarrow LUMO + 1, HOMO - 2 \rightarrow LUMO + 1 and HOMO \rightarrow LUMO + 2 transitions. Moreover, LUMO and LUMO + 1 orbitals are distributed on the A- π -A moiety with a large amount of distributions on the anchoring group, while the LUMO + 2 orbital is only located on the quinoxaline unit. Accordingly, except for HOMO \rightarrow LUMO + 2 transition (in band III), all other electronic transitions can carry electrons to LUMO and LUMO + 1 orbitals, which are overlapped with the anchoring group. Therefore, these efficiently absorbed photons from each of the three absorption bands are preferable to the intramolecular charge separation and electron injection. As a result, the quinoxaline unit is an ideal electron-withdrawing unit for constructing high performance D-A- π -A organic sensitizers. It is beneficial to obtain high J_{sc} , V_{oc} and η as well as stability by proper molecular modulation. Notably, some quinoxaline-based dyes with common I^-/I_3^- based electrolyte have already shown efficiency higher than 9.4% in our latest research.

More recently, quinoxaline-based D-A- π -A sensitizers have been further studied by Wang *et al.*⁴⁷ and Li *et al.*⁴⁸ Wang *et al.* continued to optimize the above-mentioned structure **19** by replacing the double bond between triphenylamine and quinoxaline with a thiophene unit and introducing alkyl or alkoxy chains onto the donor or thiophene parts. A high efficiency of 8.27% (liquid DSSCs) and 7.14% (quasi-solid state DSSCs) was

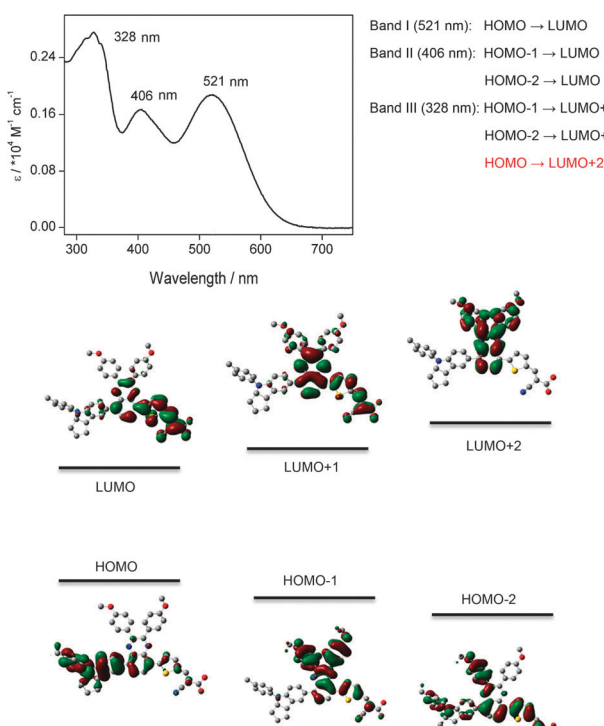


Fig. 18 Absorption spectra and TD-DFT (DFT) calculation of sensitizer **IQ1**.

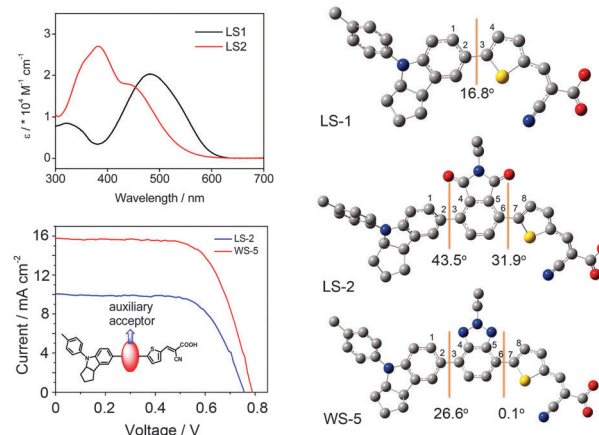


Fig. 19 Absorption spectra of **LS-2** vs. **LS-1**, photovoltaic performances of phthalimide based **LS-2** vs. **WS-5**, and the optimized configuration of **LS-1**, **LS-2** and **WS-5**. Note: in contrast with **LS-1** and **WS-5**, the indoline donor and thienyl unit in **LS-2** are rotated with respect to the phthalimide core (43.5° and 31.9° , respectively) due to the steric hindrance of the carbonyl groups from phthalimide.

obtained with the quinoxaline-based sensitizers.⁴⁷ Also, Li *et al.* employed a phenanthrene-fused quinoxaline as the additional acceptor to construct novel D-A- π -A sensitizers. An overall conversion efficiency of 7.18% was achieved under standard global AM 1.5 solar light conditions.⁴⁸

Phthalimide, which contains a couple of carbonyl groups, should endow strong electron-withdrawing capability. Moreover, the imide nitrogen also provides structural modification sites. Hence we incorporated the phthalimide unit to construct a D-A- π -A featured organic sensitizer **LS-2** (Fig. 17).⁴⁹ The CT absorption band of **LS-2** is unexpectedly blue-shifted to even shorter than **LS-1** (Fig. 5). DFT simulation indicates that the indoline donor and thienyl unit are rotated with respect to the phthalimide core (43.5° and 31.9° , respectively) due to the steric hindrance of the carbonyl groups from phthalimide (Fig. 19). Considering the very similar structure of phthalimide and benzotriazole units, we carefully compared photovoltaic performances of sensitizers **WS-5** and **LS-2**. Under the same conditions, **WS-5** shows an η of 8.38%, which is much higher than **LS-2** ($\eta = 5.11\%$) with less efficient photovoltaic parameters ($J_{sc} = 10.06 \text{ mA cm}^{-2}$, $V_{oc} = 748 \text{ mV}$, FF = 0.68). Indeed, the introduction of the phthalimide unit in **LS-2** neither expands the spectral response nor improves the photovoltage, indicating that the phthalimide unit is not suitable for constructing high efficiency D-A- π -A sensitizers. Therefore, the results demonstrate that it is essential to choose a proper subsidiary withdrawing unit in the D-A- π -A featured configuration for DSSCs.

Recently, Wang *et al.* have reported D-A- π -A featured sensitizers **21** and **22** (Fig. 20) with a thieno[3,4-*c*]pyrrole-4,6-dione (TPD) as the additional electron withdrawing unit.⁵⁰ The effect of the TPD unit on absorption spectra is sensitive to the electron donor. Compared to reference dye (terthiophyl as the π -bridge), the TPD unit does not lead to a significant red-shift of the CT band in triphenylamine-based sensitizer **21** (λ_{max} : 485 nm), while it significantly broadens the absorption

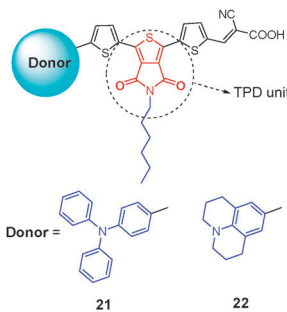


Fig. 20 Chemical structures of TPD-based D-A- π -A sensitizers **21** and **22**.

band in julolidine-based sensitizer **22** (λ_{max} 510 nm). In DSSCs, the incorporation of the TPD unit into the dye skeleton appears to retard charge recombination at the TiO_2 /dye/electrolyte interface, leading to a higher open-circuit voltage. However, the photocurrent of DSSCs based on TPD sensitizers is not enhanced due to the negligible improvement in spectral response. The spectral response and photocurrent of DSSCs based on sensitizers **21** and **22** are not improved but even decreased. Again, in agreement with the above-mentioned phthalimide unit, the TPD unit in **21** and **22** can twist molecular planarity between the electron donor and the anchoring group, possibly arising from the steric hindrance of carbonyl groups in the TPD unit.

Diketo-pyrrolopyrrole (DPP) and thienopyrazine based D-A- π -A featured organic sensitizers

DPP is a strong electron-withdrawing unit due to the presence of two lactams. As traditional pigments, DPP-based materials often show strong fluorescence with exceptional stability, thus being explored extensively in organic electronics. Tian *et al.*⁵¹ reported DPP-based organic sensitizers (**23** and **24** in Fig. 21) for DSSCs containing methoxy substituted triphenylamine as an electron donor and cyanoacrylic acid as an electron acceptor and anchoring group. The electron-withdrawing DPP unit is involved in the π -bridge between the donor and acceptor, indicative of a typical D-A- π -A configuration.

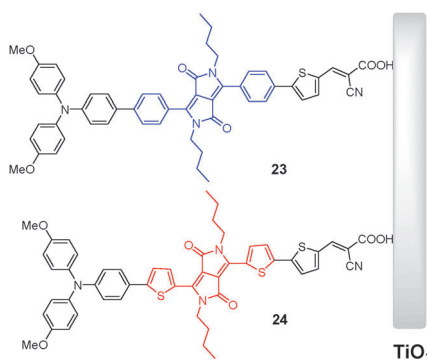


Fig. 21 Chemical structures of DPP-based D-A- π -A sensitizers **23** and **24**.

Table 4 Photophysical and photovoltaic performances of DSSCs based on DPP- and thienopyrazine-containing organic sensitizers

Dye	CT band/nm	E_{0-0}/eV	$J_{\text{sc}}/\text{mA cm}^{-2}$	V_{oc}/mV	FF	$\eta/\%$	Ref.
23	524 ^a	1.65	9.36	572	0.64	3.44	51
24	627 ^a	1.55	1.39	459	0.67	0.43	51
25	525 ^a	1.95	12.43	597	0.60	4.43	52
26	511 ^a	2.01	14.53	625	0.66	6.03	52
27	514 ^a	1.94	11.05	690	0.68	5.18	53
28	526 ^a	1.88	13.40	760	0.73	7.43	53
29	493 ^a	2.24	9.71	625	0.737	4.47	54
30	503 ^a	2.25	1.30	485	0.701	0.44	54
31	509 ^a	1.97	9.57	455	0.58	2.68	55
32	521 ^a	1.90	3.36	318	0.48	0.51	55
33	596 ^b	1.61	11.29	470	0.69	3.66	59
34	625 ^b	1.64	16.24	480	0.68	5.30	59
35	612 ^b	1.64	14.66	480	0.70	4.93	59

^a In CH_2Cl_2 . ^b In toluene.

The main difference between **23** and **24** is the aromatic rings near the DPP core (phenyl for **23** and thiophenyl for **24**). However, such a small variation in the π -conjunction of the two dyes brings a huge difference in their absorption spectra. In CH_2Cl_2 , **23** shows a CT absorption band at 524 nm, while **24** extends this band to 627 nm (Table 4). Studies on energy levels demonstrate that the bisthiophenyl bridge in **24** greatly downward shifts its LUMO level, which is 0.31 eV lower than that of **23**. When adsorbed onto the TiO_2 films, both dyes show significant aggregation with a red-shift of their CT band, meaning that the butyl chains attached on DPP units are not efficient in suppressing the intermolecular interaction. Although dye **24** exhibits a broader light-harvesting range than **23**, **24**-based DSSCs show much lower solar-to-electrical conversion efficiencies than **23** due to the mismatch between the LUMO energy level and the conduction band edge of TiO_2 .

Considering the overly decreased HOMO-LUMO gap by dithienyl fused DPP, Hua *et al.* fixed the diphenyl-DPP assembly in the π -bridge and altered the π -linker between DPP and the anchoring group to further tune the molecular energy levels.⁵² Two new π -linkers, *i.e.* furyl and phenyl, were introduced, instead of the thiophenyl unit in aforementioned **23** (Fig. 22).

Intriguingly, these sensitizers also show three major prominent absorption bands in CH_2Cl_2 , which is very similar to the BTD and quinoxaline based D-A- π -A dyes discussed above (Fig. 18). The middle band is attributed to the $\pi-\pi^*$ transition of DPP with neighboring π -spacer groups. As expected, thiophenyl and furyl based **23** and **25** show very similar CT bands at 524

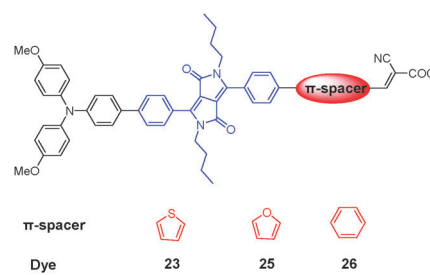


Fig. 22 Chemical structures of DPP-based D-A- π -A sensitizers **23**, **25** and **26**.

and 525 nm, indicative of a similar HOMO–LUMO gap. However, both HOMO and LUMO levels of **25** shift to the negative direction by around 0.2 eV with respect to **23**, allowing higher electron injection driving force for **25**. Among the three sensitizers, phenyl-linked **26** possesses the highest LUMO level, showing much shorter wavelength in the CT band (511 nm).

In liquid electrolyte based DSSCs, **25** and **26** show higher solar energy conversion efficiency than **23** due to higher electron injection driving force (Table 4). Especially, **26** gives better performance than **25** due to higher V_{oc} , resulting from controlled dark current. However, the performance of **25** and **26** was reversed in ionic liquid electrolyte based DSSCs. It might be shown that dye **26** with low extinction coefficient cannot absorb sufficient photons in relatively thin TiO₂ film for ionic liquid electrolyte DSSCs. The more suitable energy levels as well as higher extinction coefficient of **25** demonstrate that introducing a furyl as a π -linker is successful in constructing high efficiency DPP-based organic sensitizers. Therefore, the diphenyl-DPP-furyl π -bridge dyes **27** and **28** (Fig. 23) were specifically developed with a different donor group.⁵³

27 and **28** in CH₂Cl₂ also show three absorption bands at 300, 400 and 500 nm. The CT bands of the three dyes in Fig. 23 lie in the sequence of **27** (514 nm) < **25** (525 nm) ≈ **28** (526 nm), indicating that the contribution of the donor part to the CT band wavelength increases in the sequence of triphenylamine (TPA) < methoxy substituted triphenylamine (MeOTPA) ≈ indoline. Compared with the TPA donor, both MeOTPA and indoline further optimize energy levels by means of decreasing the HOMO–LUMO gap and shifting the HOMO and LUMO values to the negative direction (Fig. 23), which not only enhance the light-harvesting range of sensitizers, but also

increase the electron injection driving force with the promise of sufficient dye regeneration driving force. On the other hand, to avoid the serious aggregation of DPP based sensitizers, branched long alkyl chains were introduced into dye **28**. As a result, **28** based DSSCs gave a high J_{sc} of 13.40 mA cm⁻², a V_{oc} of 0.76 V and an η of 7.43% under standard AM1.5 conditions.⁵³ Importantly, such solar cell devices show excellent stability after a long period of observation. Accordingly, the systematic molecular engineering of the π -bridge and the donor part gradually increases the efficiency of DPP-based DSSCs from 1.45% to 7.43%, demonstrating its pivotal role in the molecular modulation of photovoltaic performances.

Besides the traditional D–A– π –A configuration, there are also some special assemblies of DPP-based organic sensitizers, such as A– π –A and D– π –A– π –D configurations. Odobel *et al.* reported two DPP-based organic dyes **29** and **30** (Fig. 24) by removing the traditional arylamine electron donor.⁵⁴ DFT simulation indicates that the HOMO orbitals of both dyes are localized at the DPP core, while the LUMO orbitals distribute across the entire A– π –A unit. The electron deficient nature of the DPP unit increases the oxidation potential. Consequently, both HOMO and LUMO levels sink to the positive direction, resulting in low electron injection driving force and excessive dye regeneration driving force. The J_{sc} of both dye based DSSCs is extremely sensitive to the presence of 4-*tert*-butylpyridine (TBP) in the electrolyte, further confirming the weak electron injection process. Definitely, the electron-rich donor group is very necessary for the reasonable construction of organic sensitizers.

Hua *et al.* designed two D– π –A– π –D featured organic sensitizers based on the DPP unit (**31** and **32** in Fig. 24).⁵⁵ TPA and MeOTPA were grafted onto the phenyl-extended terminal of DPP as electron donors, and a carboxylic acid was introduced into one of the lactam of DPP, serving as an anchoring group. Such a dye configuration is expected to exhibit good photovoltaic

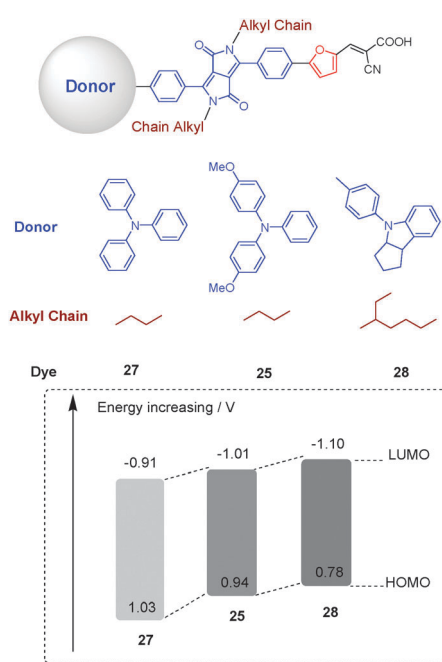


Fig. 23 Chemical structures and HOMO–LUMO levels of DPP-based D–A– π –A sensitizers **25**, **27** and **28**.

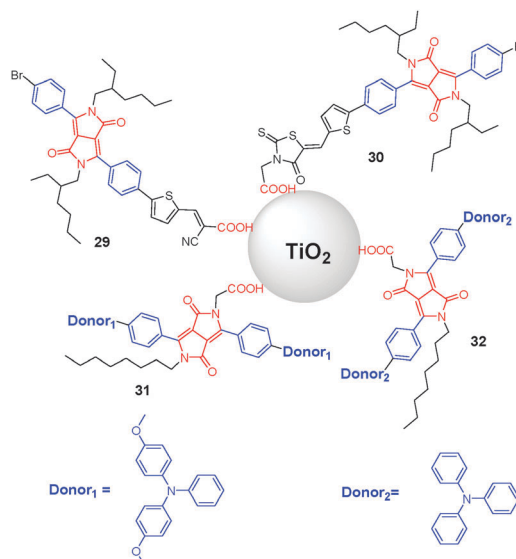


Fig. 24 Chemical structures of DPP-based sensitizers **29**–**32**.

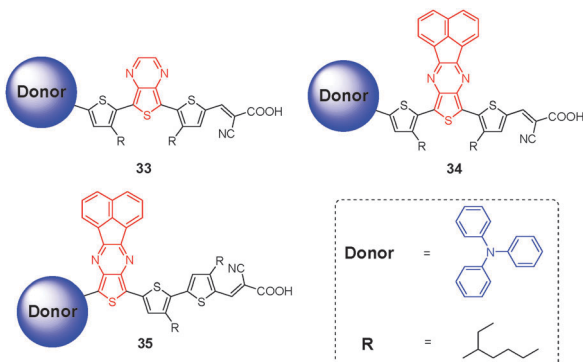


Fig. 25 Chemical structures of thienopyrazine-based D-A- π -A sensitizers 33–35.

performances in that the electrons can flow from two terminal electron donors to the core acceptor moiety. However, both dyes show pretty low performance in overall conversion efficiency (<3%). We attribute the low photovoltaic performances of two D- π -A- π -D dyes 31 and 32 to the following reasons: (i) such a molecular steric configuration inevitably makes the donor part close to the TiO₂ surface, thus essentially accelerating the injected electron recombination from the TiO₂ conduction band to the oxidized dye;¹⁰ (ii) the undesirable methylene in the anchoring group ($-\text{CH}_2\text{CO}_2\text{H}$) is unconjugated to the dye skeleton, which potentially separates electron orbital coupling between the sensitizer and TiO₂. With the less electronic coupling, the photo-excited electrons can not inject deeply into TiO₂ nanoparticles and accelerate the charge recombination between photo-injected electrons and the oxidized dyes, thus resulting in relatively low efficiency.^{56,57}

Thieno[3,4-*b*]pyrazine is also a strong electron-withdrawing unit.⁵⁸ Wang *et al.* introduced the thieno[3,4-*b*]pyrazine unit into the backbone of organic sensitizers (33–35 in Fig. 25).⁵⁹ Essentially, these dyes are also classified as D-A- π -A configuration dyes, and the electron-withdrawing thieno[3,4-*b*]pyrazine can greatly red-shift their absorption bands to the real near-infrared (NIR) region. These dyes show absorption maxima at 596–625 nm with the threshold above 800 nm. Dye 34 shows the longest CT band (λ_{max} 625 nm) due to the π -extension in the thienopyrazine spacer and the proper linking groups. Impressively, the IPCE onset of dye 34 based DSSCs is extended above 900 nm, which is even comparable to that of the black dye. After careful optimization with the concentration of I₂ and TBP in a polymer gel electrolyte system, 34 based quasi-solid state DSSCs gave the power conversion efficiency as high as 5.30%. Presently, this is very promising efficiency for quasi-solid state DSSCs based on organic NIR dyes.

As listed in Table 4, the DPP-based dye 24 and thienopyrazine-based dye 34 show similar narrow HOMO-LUMO energy gaps of 1.5–1.6 eV and maximal absorption peaks at above 620 nm in organic solvents. It is strongly recommended that the tuning of spectral response of organic sensitizers to the NIR region can be readily realized by incorporation of proper electron-withdrawing units into the molecule skeleton. However, their huge difference in DSSC performances reminds us that the

fine modulation of energy levels of HOMO and LUMO orbitals is of critical importance to low energy gap sensitizers.

Thiazole, bithiazole and triazine based D-A- π -A featured organic sensitizers

Thiazole is a common moderate electron-withdrawing heterocycle. Several moieties based on thiazole have been widely introduced into organic semiconductors, with high performances in organic electronic devices.⁶⁰ Sensitizers 36 and 37 (Fig. 26) contain a thiazolyl unit in the π -conjugation.⁶¹ Note that the nitrogen atom of the thiazolyl unit is placed at different positions for these two dyes. Compared to a thienyl based analogue, the thiazole unit in both dyes decreases the HOMO-LUMO gap, and red-shifts the CT band by more than 20 nm. As found, the photovoltaic performance of 36 is better than that of 37. Therefore, the linking manner of the thiazolyl unit in the conjugation bridge is critical to the photovoltaic performances of 36 and 37. Moreover, it is worth getting further insight into the fact that 36 can realize better photovoltaic performance.

Recently, Tian and Hua *et al.* developed a series of organic sensitizers 38–42 by incorporating a bithiazole unit into the π -linker.⁶² They carefully modified the electron donor and π -bridge by introducing the methoxy group, phenyl group, and triple bond for tailoring their combination pattern. As demonstrated, since the phenyl as a π -linker is unfavorable to extend the CT band, sensitizer 39 shows the longer CT band at 460 nm relative to 40. As listed in Table 5, DSSCs based on these five dyes exhibit high V_{oc} (745–810 mV) with a moderate conversion efficiency (in the range of 4.20–5.73%).

Apparently, due to their relatively weak electron-withdrawing character, thiazole and bithiazole-based organic D-A- π -A dyes do not show broad spectral response. All these dyes (36–42) show the HOMO-LUMO gap greater than 2.3 eV, and the CT band shorter than 465 nm. However, it is worth replacing the thienyl unit with the thiazolyl unit in some

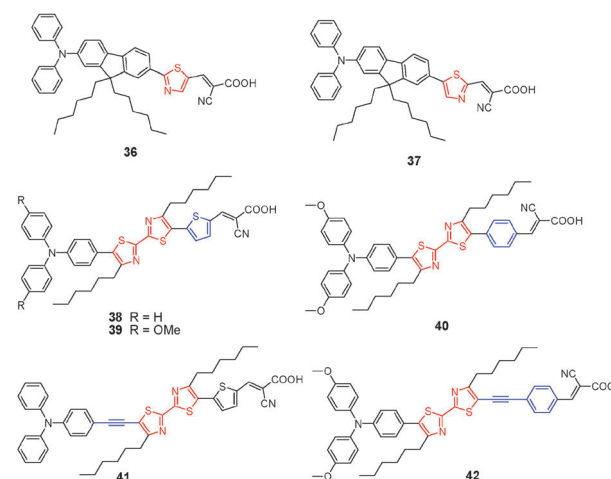


Fig. 26 Chemical structures of thiazole- and bithiazole-based sensitizers 36–42.

Table 5 Photophysical and photovoltaic performances of DSSCs based on thiazole-, bithiazole- and triazine-containing D-A- π -A featured organic sensitizers

Dye	CT band/nm	E_{0-0}/eV	$J_{sc}/\text{mA cm}^{-2}$	V_{oc}/mV	FF	$\eta/\%$	Ref.
36	448 ^a	2.33	14.55	710	0.67	6.88	61
37	452 ^a	2.32	10.40	660	0.72	4.92	61
38	457 ^b	2.42	11.78	810	0.60	5.73	62
39	460 ^b	2.37	10.22	745	0.59	4.48	62
40	410 ^b	2.48	8.92	782	0.60	4.20	62
41	465 ^b	2.38	12.06	754	0.62	5.60	62
42	426 ^b	2.53	10.51	790	0.61	5.05	62
43	396 ^c	2.48	3.33	757	0.718	1.81	63
44	403 ^c	2.39	1.67	648	0.759	0.82	63

^a In THF. ^b In CH_2Cl_2 . ^c In N,N -dimethylformamide (DMF).

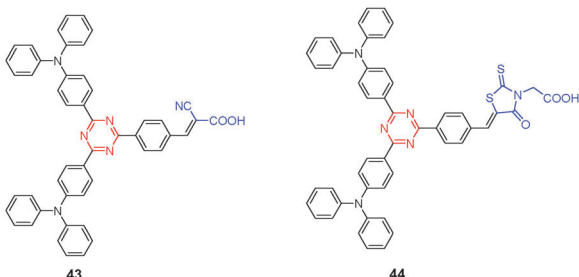


Fig. 27 Chemical structures of triazine-based D-A- π -A sensitizers 43 and 44.

reported high performance sensitizers (such as aforementioned WS-2) because it seems extremely beneficial to high V_{oc} .

Li *et al.* designed a series of organic dyes by incorporation of an electron-withdrawing triazine as the π -spacer.⁶³ Two of them (43 and 44) are shown in Fig. 27. Although triazine is a strong electron-withdrawing unit, it does not contribute to the red-shift of the absorption band of dyes 43 and 44. Disappointedly, both dyes show very short CT bands below 400 nm, possibly arising from the unbeneficial linking manner with triazine. That is, the *meta*-position bridged with the electron donor and acceptor on the triazine core cannot form a preferable resonance, resulting in the exactly weak delocalization over the dye molecule. As a result, the power conversion efficiencies for dyes 43 and 44 are rather low due to the limited photocurrent response and unfavorable charge transfer process.

Cyano- and fluoro-based D-A- π -A featured organic sensitizers

On the basis of the D- π -A model, Hara *et al.* have reported a series of coumarin dyes by using a different number of thiophene and/or methine units as π -conjugation bridges.^{64,65} Given that it is difficult to further extend spectral response to the longer wavelength region *via* simply increasing the number of π -conjugation units, Wang and Hara *et al.* introduced a cyano ($-\text{CN}$) group into the π -conjugation bridge of coumarin dye 45, resulting in 46 and 47 (Fig. 28) with successfully extending the photoresponse to longer wavelengths.^{66,67} Here, dye 46 can also be regarded as a representative of a typical series of D-A- π -A

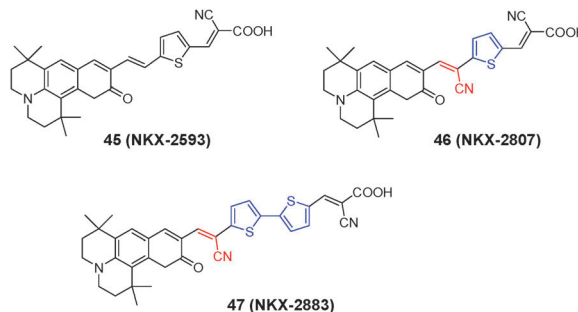
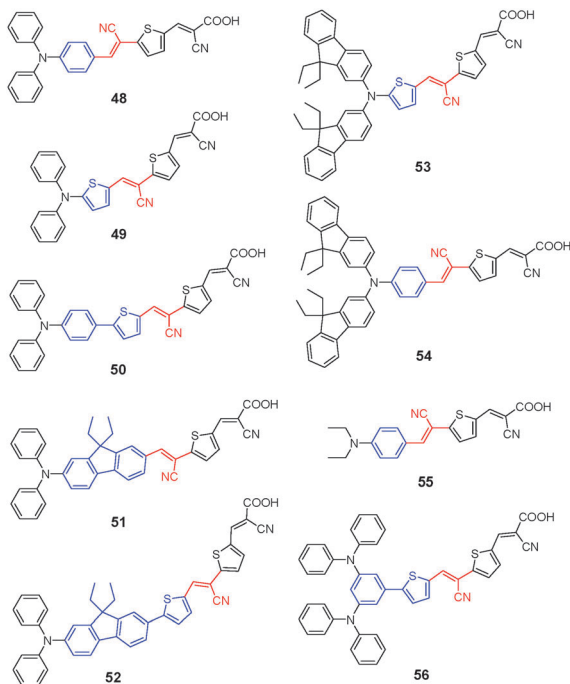
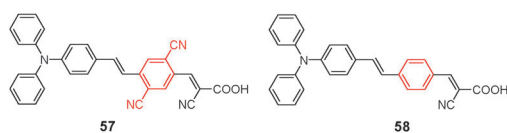


Fig. 28 Chemical structures of cyano-based sensitizers 45–47.

featured sensitizers constructed with a cyano group rather than a heterocyclic ring. Dye 45 shows its CT band at 510 nm, while incorporation of the cyano group in 46 red-shifts its CT band to 566 nm. Obviously, the internal electron-withdrawing cyano group can distinctly decrease the gap between HOMO and LUMO orbitals. When the additional cyano group is separated by two thiényl units (47), the CT band is unexpectedly blue-shifted from 566 to 552 nm. As a result, the incorporated cyano group can preferably facilitate the electron-transfer from the coumarin donor to the anchoring group of cyanoacrylic acid, but such an enhancement may become weak if the cyano group is far away from the cyanoacrylic acid. Nevertheless, dye 47 shows a very high molar extinction coefficient of $97\,400 \text{ M}^{-1} \text{ cm}^{-1}$ with the almost same onset as 46 on TiO_2 film. Accordingly, dye 47 realized a strikingly high J_{sc} of 18.8 mA cm^{-2} , even in a $6 \mu\text{m}$ thick TiO_2 photoanode based DSSC with a pretty good device stability. Based on these metal-free coumarin organic dyes, the long-term device stability with a power-conversion efficiency of *ca.* 6% was realized, and operated for up to 1000 h under continuous light-soaking stress.

Lin *et al.* also reported a series of arylamine-based organic dyes 48–56 with an incorporated cyano group in the π -conjugation bridge.⁶⁸ Similarly, the additional cyano group in these dyes also plays an important role in the red-shifting of the absorption band. For instance, dye 48 has a much larger λ_{\max} value than the analogous without the incorporated cyano group (478 nm vs. 444 nm in MeOH).⁶⁹ Similarly, the λ_{\max} value of 51 is also red-shifted by 60 nm with respect to that of the corresponding cyano-free analogues.⁷⁰ They systematically tailored the π -linker including phenyl, thiényl and fluorenyl units. However, the photovoltaic performances based on these dyes are moderate, in the range of 3.38–4.92% (Fig. 29).

The cyano group in sensitizers 46–56 is grafted on a vinylene unit. Besides, Sun *et al.* introduced two cyano groups attached on a phenylene unit in the π -bridge of dye 57 (Fig. 30).⁷¹ Such structural modification also decreases the HOMO-LUMO gap with a large red-shift by 62 nm in the CT absorption band with respect to that of the cyano-free analogues (dye 58). Moreover, the LUMO orbital of dye 57 shows a similar electron distribution to that of reference dye 58, in which the electron is delocalized at the cyanoacrylic acid unit and the phenylene subunit. The good overlap between the HOMO and the LUMO in 57 can assure the photo-induced electron injection from the

**Fig. 29** Chemical structures of cyano-based sensitizers 48–56.**Fig. 30** Chemical structures of dicyano-substituted sensitizer 57 and reference dye 58.

electron donor of the triphenylamine unit into the dicyano-substituted phenylene subunit, then into the cyanoacrylic acid segment, and finally into the conduction band of TiO_2 . Obviously, consistent with the above-mentioned D-A- π -A featured sensitizers constructed with electron-withdrawing heterocyclic rings such as BTD and quinoxaline units, two cyano groups on the phenylene subunit can be still treated as an “electron trap” to assist the electron transfer from the electron donor to the anchoring group, resulting in a large red-shift of the absorption band. Accordingly, we can rule out the possibility that the electron-withdrawing substituent on the phenylene subunit is the barrier to the electron injection into the conduction band of TiO_2 . However, the DSSC based on dye 57 exhibited a rather low photon-to-electron conversion efficiency (0.44%, Table 6). This might be attributed to the distinct decrease in molar extinction coefficients (ϵ , $12\,000\text{ M}^{-1}\text{ cm}^{-1}$ in CH_2Cl_2) of dye 57 upon introduction of two cyano groups on the phenylene subunit, resulting in the dissatisfaction light-harvesting efficiency with a critically lower photocurrent.⁷¹ Moreover, in dye 57, the dicyano-substituted phenylene subunit is directly connected to the anchoring group of cyanoacrylic acid, which might result in unbeneficial fast recombination with injected electrons in TiO_2 . Considering the

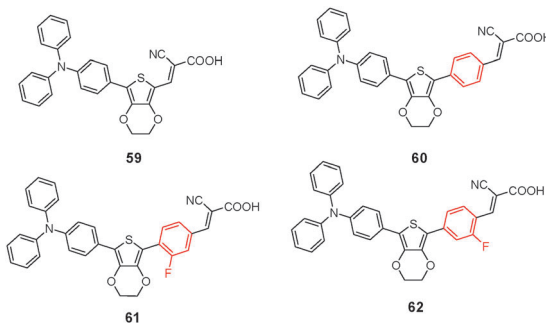
Table 6 Photophysical and photovoltaic performances of DSSCs based on cyano- and fluoro-containing D-A- π -A featured organic sensitizers

Dye	CT band/nm	E_{0-0}/eV	$J_{sc}/\text{mA cm}^{-2}$	V_{oc}/mV	FF	$\eta/\%$	Ref.
45	510 ^a	1.82	14.89	580	0.73	6.3	67
46	566 ^a	1.68	10.93	530	0.75	4.3	67
47	552 ^a	1.69	18.8	530	0.65	6.5	66
48	478 ^b	2.09	11.40	590	0.64	4.28	68
49	524 ^b	1.86	13.43	570	0.64	4.92	68
50	498 ^b	1.97	11.43	560	0.65	4.15	68
51	482 ^b	2.07	11.00	580	0.69	4.34	68
52	505 ^b	1.90	9.56	550	0.66	3.48	68
53	560 ^b	1.76	11.96	580	0.65	4.51	68
54	511 ^b	1.93	12.48	610	0.64	4.81	68
55	505 ^b	1.98	11.56	560	0.62	4.04	68
56	463 ^b	—	9.24	550	0.68	3.48	68
57	500 ^c	2.11	1.3	480	0.70	0.44	71
58	438 ^c	2.33	9.7	760	0.72	5.33	71
59	426 ^d	2.53	15.5	690	0.683	7.30	72
60	420 ^e	2.47	14.73	754	0.65	7.25	73
61	440 ^e	2.37	15.78	735	0.60	7.00	73
62	420 ^e	2.53	15.58	787	0.67	8.22	73
63	450 ^d	—	6.79	830	0.65	3.69 ^f	75
64	460 ^d	—	7.52	910	0.71	4.86 ^f	75
65	462 ^c	2.30	13.5	702	0.68	6.4	76
66	430 ^c	2.56	10.5	672	0.68	4.8	76

^a In ethanol. ^b In THF. ^c In CH_2Cl_2 . ^d In *tert*-butanol-acetonitrile (1 : 1) solution. ^e In DMF. ^f Photovoltaic performances of solid-state DSSCs.

case of dyes 13 and 14 reported by Bäuerle *et al.*,³⁴ the incorporated electron acceptor of the dicyano-substituted phenylene subunit should be placed away from the anchoring group by a rigid linker to block the electron recombination between TiO_2 and dye cations.

Nowadays, fluorine chemistry is very popular in the area of organic functional materials due to its unique chemical properties. Several groups have incorporated fluorine element into the structure of organic sensitizers. It is found that the electron-withdrawing character and resonance effect of fluorine simultaneously affect the properties of fluoro-based sensitizers. Chou *et al.* reported a simple organic sensitizer 59,⁷² which shows very promising performance ($\eta = 7.3\%$) though its CT absorption band is located only at a short wavelength of 426 nm in *tert*-butanol-acetonitrile (v/v, 1 : 1). To expand the photo-response of sensitizer 59, they chose a facile approach by incorporating a phenyl unit in the absence/presence of fluorine substitution to elongate the π -conjugation length, resulting in dyes 60–62.⁷³ Considering the electron-withdrawing character of the fluorine group in the π -bridge, sensitizers 61 and 62 can also be treated as typical D-A- π -A configuration sensitizers. However, their results indicate that elongation of the π -bridge by a phenyl group shows little contribution to broaden spectral response (Table 6). Moreover, the substitution position of the fluorine atom on the phenyl bridge has a different effect on the CT absorption band to some extent. Given that both dyes 60 and 62 show the CT band at 420 nm, in reference to the position of the anchoring group (acrylic acid), the *ortho*-fluoro substitution in 62 does not lead to any red-shift of the CT absorption band due to the concerted offset between inductive and resonance effects of the fluorine atom. Actually, among four halogen elements, fluorine is the least deactivating, and

**Fig. 31** Chemical structures of sensitizers 59–62.

fluorobenzenes usually show reactivity approximating that of benzene itself, with the *ortho*-*para* orientation effect.⁷⁴ In contrast with **60** and **62**, the CT absorption band of **61** exhibits a red-shift by 20 nm due to the *meta*-fluoro inductive effect on the cyanoacrylic acid unit, where the electron withdrawing property of the fluorine atom lowers the LUMO energy, resulting in the smallest energy gap among the four sensitizers.⁷³ Unexpectedly, in DSSCs, sensitizer **62** with a short absorption band shows higher performance than **60** and **61** mainly due to its higher V_{oc} (787 mV). Moreover, the resonance conjugation between *ortho*-fluorine and anchoring groups in **62** seems beneficial for improving the dye loading amount (fluorine increases the ligand basicity and hence the TiO₂ affinity), resulting in a single compacted dye layer to decrease unfavorable charge recombination. Accordingly, the *ortho*-fluoro group in **62** assures better charge transport from the electron donor to the anchoring acceptor, then to TiO₂ than that of **60** and **61**. In addition, it is suspected that the *ortho*-fluoro group in **62** might negatively shift the conduction band of TiO₂ because of its dipole moment (negative site) pointing toward the TiO₂ surface.⁷³ Overall, this work nicely manifests the importance of fluorine substitution in DSSC performances, which can be attributed to the specific inductive *vs.* resonance concerted effects on the D-A strength as well as electronic coupling with nanostructured TiO₂ to a different extent (Fig. 31).

Encouraged by the concerted effects of the fluorine atom, Chou *et al.* also developed another fluoro-based sensitizer **64** (Fig. 32)⁷⁵ with a cyclopentadithiophene in the π -bridge for

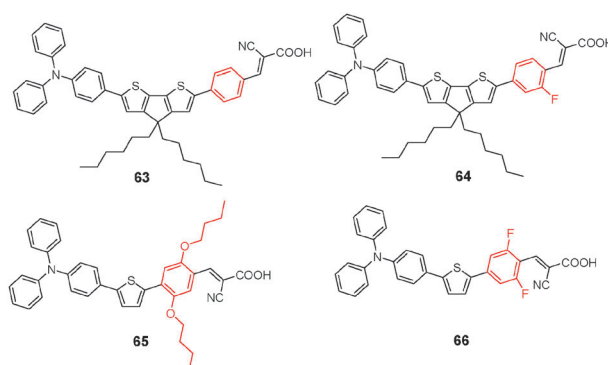
overcoming the short wavelength response of **62**. In contrast with the EDOT unit in **60** and **62**, the cyclopentadithiophene in **63** and **64** efficiently increases the conjugation length, exhibiting the CT absorption band at 450 and 460 nm, respectively. Here, the 10 nm red-shift of the CT band of **64** relative to **63** can be definitely ascribed to the incorporated fluoro group on the *ortho*-position relative to the anchoring group (acrylic acid). Both dyes **64** and **63** show high extinction coefficients ($>50\,000\text{ M}^{-1}\text{ cm}^{-1}$ at λ_{max}), especially suitable for application in solid state DSSCs, which consist of a very thin TiO₂ anode (1.6 μm thickness) and a solid state hole conductor (*spiro*-MeOTAD). In solid state DSSCs, sensitizer **64** gives a high V_{oc} of 910 mV and an efficiency of 4.86%.⁷⁵ Again, it is encouraging that the *ortho*-fluoro substituent in **64** attracts the lithium ion to a position adjacent to the TiO₂ surface, thus increasing the electron diffusion length in TiO₂ with better electron collection. The contribution of these two factors should account for the increase of V_{oc} as well as the overall cell performance.

Wang *et al.* carefully compared alkoxy- or fluoro-substitution on the phenyl unit in a triphenylamine based organic sensitizer (Fig. 32).⁷⁶ In this work, the alkoxy-substituted **65** shows better performance than difluoro-substituted **66** due to its broader spectral response. The difluoro-substituted **66** gives the CT band at 430 nm, which is blue-shifted by 32 nm with respect to **65**. As expected, DFT simulation indicates that the *ortho*-difluoro substitution in **66** increases the twist between phenyl and anchoring cyanoacrylic acid (33.2°),⁷⁶ thus breaking the molecular planarity and conjugation. As mentioned above, since the phenyl-bridge itself is unfavorable to the molecular planarity of sensitizers, the steric hindrance induced by the difluoro-substitution on the phenyl group should be seriously taken into consideration.

Conclusions

Light absorption from the visible to the NIR region is a precondition to increase the photocurrent and photo-energy conversion efficiencies in DSSCs. We have systematically described the promising design of organic sensitizers from the traditional D- π -A to D-A- π -A feature for high-performance DSSCs (Fig. 33), especially focusing on additional electron acceptors. To distinguish the feature from the traditional D- π -A and emphasize the role of incorporated electron-withdrawing acceptors, we specifically name these dyes D-A- π -A configuration dyes. The electron-withdrawing building blocks (such as BTP, benzotriazole, quinoxaline, phthalimide, DPP, thienopyrazine, thiazole, triazine, cyanovinyl, cyano- and fluoro-substituted phenyl) have been taken into account in the π bridge as internal acceptors for D-A- π -A sensitizers, which realize several merits:

(i) In the D-A- π -A featured configuration, insertion of an additional electron-withdrawing unit into the π -bridge can red-shift the CT absorption band, and efficiently modulate the molecular optical band-gap. Specifically, incorporation of the DPP or thienopyrazine unit can readily extend the CT band to >600 nm, even being capable of developing NIR dyes. The unit of BTD, quinoxaline and cyano group can move the CT band

**Fig. 32** Chemical structures of sensitizers 63–66.

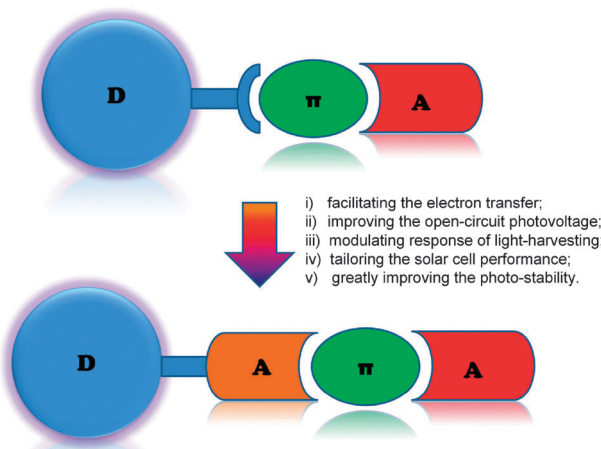


Fig. 33 Organic sensitizers from the D- π -A to the D-A- π -A featured configuration for high-performance DSSCs.

into the range of 500–600 nm, realizing an ideal orbital match with the TiO₂ conduction band and I[−]/I₃[−] redox couples. As units with weak electron-withdrawing properties, the benzotriazole, thiazole and fluoro-substituted phenyl group result in a slight red-shift of the CT band (always below 500 nm). Due to the steric hindrance of carbonyl groups from phthalimide, the introduction of the phthalimide unit in LS-2 might make the molecular configuration twist in less planarity, with little expansion of its spectral response. Therefore, it is essential to choose the proper subsidiary withdrawing unit in the D-A- π -A featured configuration for DSSCs. Accordingly, we can easily tune the light-harvesting response in the visible and the NIR region by exploring different electron-withdrawing units in D-A- π -A dyes. Of course, the suitable electron donor, π -linker and anchoring group are necessary for further spectral modulation.

(ii) Generally, more than 0.2 eV potential differences are necessary for driving electron transfer from the dye's LUMO to TiO₂, and from the redox couple in the electrolyte to oxidized dye. For typical DSSCs based on I[−]/I₃[−] redox couples, the low band-gap of sensitizers is beneficial for harvesting more solar light. But the HOMO-LUMO band-gap should be well controlled. In D-A- π -A featured organic sensitizers, the additional acceptor unit provides a facile channel for tuning and controlling HOMO-LUMO levels.

(iii) Note that the presence of two acceptors in D-A- π -A does not mean that two discrete, spatially separated LUMO orbitals are present in the system. In fact, the electron of the LUMO orbital is evenly delocalized across the entire A- π -A system, indirectly suggesting that the incorporated additional strong electron-withdrawing acceptor can serve as an “electron trap” by facilitating electron transfer from the donor to the internal acceptor/anchor (*i.e.* the cyanoacetic acid unit). DFT simulation indicates that for D-A- π -A featured dyes, their HOMO and LUMO orbitals are distributed on a large conjugated area, and distinctly overlapped with the additional acceptor unit. It is well known that electron transitions easily occur between overlapped orbitals, indicating that in the D-A- π -A configuration

the cascaded electron withdrawal from D to internal A, then to terminal A may benefit electron transfer in organic sensitizers.

(iv) As is well known, the introduction of alkyl chains on the thiényl unit is effective in preventing dye aggregation and improving open-circuit voltage and power conversion efficiency. However, compared with the high stability of WS-2, we found that the photo-stability of WS-6 sensitized TiO₂ film is decreased to some extent, which might arise from the easy oxidation of the *n*-hexyl chain on the thiényl unit. The introduced electron-withdrawing units not only serve as additional acceptors, but also realize a facile structural modification. It is very convenient to introduce long alkyl chains on quinoxaline, benzotriazole, thienopyrazine and DPP units, instead of grafting on the thiényl unit, for achieving high V_{oc} *via* blocking the self-aggregation and reducing charge recombination.

(v) The introduction of additional electron-withdrawing units in the D-A- π -A configuration is extremely beneficial for improving photo- and thermal-stability of organic sensitizers. Especially, the low stability of indoline-based organic sensitizers can be distinctly improved by such a D-A- π -A configuration. The BTD, benzotriazole, quinoxaline and DPP based organic dyes all show high stability on TiO₂ film as well as DSSC devices.

Acknowledgements

This work was financially supported by NSFC/China, National 973 Program (2011CB808400), the Oriental Scholarship, SRFDP 200802510011, the Fundamental Research Funds for the Central Universities (WK1013002), and the Open Funding Project of State Key Laboratory of Luminescent Materials and Devices (SCUT).

Notes and references

- B. O'Regan and M. Grätzel, *Nature*, 1991, **353**, 737–740.
- A. Hagfeldt, G. Boschloo, L. Sun, L. Kloo and H. Pettersson, *Chem. Rev.*, 2010, **110**, 6595–6663.
- J. N. Clifford, E. Martinez-Ferrero, A. Viterisi and E. Palomares, *Chem. Soc. Rev.*, 2011, **40**, 1635–1646.
- N. Robertson, *Angew. Chem., Int. Ed.*, 2006, **45**, 2338–2345.
- Z. Ning, Q. Zhang, W. Wu, H. Pei, B. Liu and H. Tian, *J. Org. Chem.*, 2008, **73**, 3791–3797.
- X. M. Ren, S. H. Jiang, M. Y. Cha, G. Zhou and Z.-S. Wang, *Chem. Mater.*, 2012, **24**, 3493–3499.
- A. Mishra, M. K. R. Fischer and P. Bäuerle, *Angew. Chem., Int. Ed.*, 2009, **48**, 2474–2499.
- Y. Yen, H. Chou, Y. Chen, C. Hsu and J. T. Lin, *J. Mater. Chem.*, 2012, **22**, 8734–8747.
- Z. J. Ning and H. Tian, *Chem. Commun.*, 2009, 5483–5495.
- Z. J. Ning, Y. Fu and H. Tian, *Energy Environ. Sci.*, 2010, **3**, 1170–1181.
- C. Li and H. Wonneberger, *Adv. Mater.*, 2012, **24**, 613–636.
- K. R. Justin Thomas, J. T. Lin, M. Velusamy, Y. T. Tao and C. H. Chuen, *Adv. Funct. Mater.*, 2004, **14**, 83–90.
- J. Raimundo, P. Blanchard, H. Brisset, S. Akoudad and J. Roncali, *Chem. Commun.*, 2000, 939–940.
- M. Velusamy, K. R. J. Thomas, J. T. Lin, Y. C. Hsu and K. C. Ho, *Org. Lett.*, 2005, **7**, 1899–1902.
- W. H. Zhu, Y. Z. Wu, S. T. Wang, W. Q. Li, X. Li, J. Chen, Z. S. Wang and H. Tian, *Adv. Funct. Mater.*, 2011, **21**, 756–763.
- B. Liu, W. H. Zhu, Q. Zhang, W. J. Wu, M. Xu, Z. J. Ning, Y. S. Xie and H. Tian, *Chem. Commun.*, 2009, 1766–1768.

- 17 H. Qin, S. Wenger, M. Xu, F. Gao, X. Jing, P. Wang, S. M. Zakeeruddin and M. Grätzel, *J. Am. Chem. Soc.*, 2008, **130**, 9202–9203.
- 18 D. B. Kuang, S. Uchida, R. Humphry-Baker, S. M. Zakeeruddin and M. Grätzel, *Angew. Chem., Int. Ed.*, 2008, **47**, 1923–1927.
- 19 Y. Z. Wu, X. Zhang, W. Q. Li, Z. S. Wang, H. Tian and W. H. Zhu, *Adv. Energy Mater.*, 2012, **2**, 149–156.
- 20 Z. J. Ning, Q. Zhang, H. C. Pei, J. F. Luan, C. G. Lu, Y. P. Cui and H. Tian, *J. Phys. Chem. C*, 2009, **113**, 10307–10313.
- 21 N. Koumura, Z. S. Wang, S. Mori, M. Miyashita, E. Suzuki and K. Hara, *J. Am. Chem. Soc.*, 2006, **128**, 14256–14257.
- 22 M. Miyashita, K. Sunahara, T. Nishikawa, Y. Uemura, N. Koumura, K. Hara, A. Mori, T. Abe, E. Suzuki and S. Mori, *J. Am. Chem. Soc.*, 2008, **130**, 17874–17881.
- 23 M. Jørgensen, K. Norrman, S. A. Gevorgyan, T. Tromholt, B. Andreasen and F. C. Krebs, *Adv. Mater.*, 2012, **24**, 580–612.
- 24 J. H. Seo, A. Gutacker, Y. Sun, H. Wu, F. Huang, Y. Cao, U. Scherf, A. J. Heeger and G. C. Bazan, *J. Am. Chem. Soc.*, 2011, **133**, 8416–8419.
- 25 X. H. Zhu, J. B. Peng, Y. Cao and J. Roncali, *Chem. Soc. Rev.*, 2011, **40**, 3509–3524.
- 26 Y. F. Li, *Acc. Chem. Res.*, 2012, **45**, 723–733.
- 27 D. H. Lee, M. J. Lee, H. M. Song, B. J. Song, K. D. Seo, M. Pastore, C. Anselmi, S. Fantacci, F. De Angelis, M. K. Nazeeruddin, M. Grätzel and H. K. Kim, *Dyes Pigm.*, 2011, **91**, 192–198.
- 28 B. Liu, Q. B. Liu, D. You, X. Y. Li, Y. Naruta and W. H. Zhu, *J. Mater. Chem.*, 2012, **22**, 13348–13356.
- 29 J. Kim, H. Choi, J. Lee, M. Kang, K. Song, S. O. Kang and J. Ko, *J. Mater. Chem.*, 2008, **18**, 5223–5229.
- 30 W. Q. Li, Y. Z. Wu, X. Li, Y. S. Xie and W. H. Zhu, *Energy Environ. Sci.*, 2011, **4**, 1830–1837.
- 31 M. Xu, M. Zhang, M. Pastore, R. Li, F. De Angelis and P. Wang, *Chem. Sci.*, 2012, **3**, 976–983.
- 32 Z. M. Tang, T. Lei, K. J. Jiang, Y. L. Song and J. Pei, *Chem.-Asian J.*, 2010, **5**, 1911–1917.
- 33 S. Kim, H. Lim, K. Kim, C. Kim, T. Y. Kang, M. J. Ko and N. G. Park, *IEEE J. Sel. Top. Quantum Electron.*, 2010, **16**, 1627–1634.
- 34 S. Haid, M. Marszalek, A. Mishra, M. Wielopolski, J. Teuscher, J. Moser, R. Humphry-Baker, S. M. Zakeeruddin, M. Grätzel and P. Bäuerle, *Adv. Funct. Mater.*, 2012, **22**, 1291–1302.
- 35 Y. Z. Wu, M. Marszalek, S. M. Zakeeruddin, Q. Zhang, H. Tian, M. Grätzel and W. H. Zhu, *Energy Environ. Sci.*, 2012, **5**, 8261–8272.
- 36 R. Katoh, A. Furube, S. Mori, M. Miyashita, K. Sunahara, N. Koumura and K. Hara, *Energy Environ. Sci.*, 2009, **2**, 542–546.
- 37 M. Manceau, S. Chambon, A. Rivaton, J. Gardette, S. Guillerez and N. Lemaître, *Sol. Energy Mater. Sol. Cells*, 2010, **94**, 1572–1577.
- 38 S. C. Price, A. C. Stuart, L. Yang, H. Zhou and W. You, *J. Am. Chem. Soc.*, 2011, **133**, 4625–4631.
- 39 Z. Zhang, B. Peng, B. Liu, C. Pan, Y. Li, Y. He, K. Zhou and Y. Zou, *Polym. Chem.*, 2010, **1**, 1441–1447.
- 40 Y. Cui, Y. Z. Wu, X. F. Lu, X. Zhang, G. Zhou, F. B. Miapeh, W. H. Zhu and Z. S. Wang, *Chem. Mater.*, 2011, **23**, 4394–4401.
- 41 J. N. Clifford, E. Martinez-Ferrero and E. Palomares, *J. Mater. Chem.*, 2012, **22**, 12415–12422.
- 42 M. Zhang, J. Liu, Y. Wang, D. Zhou and P. Wang, *Chem. Sci.*, 2011, **2**, 1401–1406.
- 43 J. Y. Mao, F. L. Guo, W. J. Ying, W. J. Wu, J. Li and J. L. Hua, *Chem.-Asian J.*, 2012, **7**, 982–991.
- 44 Y. Uemura, S. Mori, K. Hara and N. Koumura, *Chem. Lett.*, 2011, **40**, 872–873.
- 45 D. W. Chang, H. J. Lee, J. H. Kim, S. Y. Park, S. M. Park, L. Dai and J. B. Baek, *Org. Lett.*, 2011, **13**, 3880–3883.
- 46 K. Pei, Y. Z. Wu, W. J. Wu, Q. Zhang, B. Q. Chen, H. Tian and W. H. Zhu, *Chem.-Eur. J.*, 2012, **18**, 8190–8200.
- 47 X. F. Lu, Q. Y. Feng, T. Lan, G. Zhou and Z.-S. Wang, *Chem. Mater.*, 2012, **24**, 3179–3187.
- 48 J. Shi, J. N. Chen, Z. F. Chai, H. Wang, R. L. Tang, K. Fan, M. Wu, H. W. Han, J. G. Qin, T. Y. Peng, Q. Q. Li and Z. Li, *J. Mater. Chem.*, 2012, **22**, 18830–18838.
- 49 W. Q. Li, Y. Z. Wu, Q. Zhang, H. Tian and W. H. Zhu, *ACS Appl. Mater. Interfaces*, 2012, **4**, 1822–1830.
- 50 Q. Y. Feng, X. F. Lu, G. Zhou and Z. S. Wang, *Phys. Chem. Chem. Phys.*, 2012, **14**, 7993–7999.
- 51 S. Y. Qu, W. J. Wu, J. L. Hua, C. Kong, Y. T. Long and H. Tian, *J. Phys. Chem. C*, 2010, **114**, 1343–1349.
- 52 S. Y. Qu, B. Wang, F. L. Guo, J. Li, W. J. Wu, C. Kong, Y. T. Long and J. L. Hua, *Dyes Pigm.*, 2012, **92**, 1384–1393.
- 53 S. Y. Qu, C. J. Qin, A. Islam, Y. Z. Wu, W. H. Zhu, J. L. Hua, H. Tian and L. Y. Han, *Chem. Commun.*, 2012, **48**, 6972–6974.
- 54 J. Warnan, L. Favereau, Y. Pellegrin, E. Blart, D. Jacquemin and F. Odobel, *J. Photochem. Photobiol. A*, 2011, **226**, 9–15.
- 55 F. L. Guo, S. Y. Qu, W. J. Wu, J. Li, W. J. Ying and J. L. Hua, *Synth. Met.*, 2010, **160**, 1767–1773.
- 56 X. M. Huang, Y. Fang, X. Li, Y. S. Xie and W. H. Zhu, *Dyes Pigm.*, 2011, **90**, 297–303.
- 57 J. Wiberg, T. Marinado, D. P. Hagberg, L. Sun, A. Hagfeldt and B. Albinsson, *J. Phys. Chem. C*, 2009, **113**, 3881–3886.
- 58 S. C. Rasmussen, R. L. Schwiderski and M. E. Mulholland, *Chem. Commun.*, 2011, **47**, 11394–11410.
- 59 X. F. Lu, G. Zhou, H. Wang, Q. Y. Feng and Z. S. Wang, *Phys. Chem. Chem. Phys.*, 2012, **14**, 4802–4809.
- 60 Y. Z. Lin, H. J. Fan, Y. F. Li and X. W. Zhan, *Adv. Mater.*, 2012, **24**, 3087–3106.
- 61 C. Chen, Y. Hsu, H. Chou, K. R. J. Thomas, J. T. Lin and C. Hsu, *Chem.-Eur. J.*, 2010, **16**, 3184–3193.
- 62 J. X. He, W. J. Wu, J. L. Hua, Y. H. Jiang, S. Y. Qu, J. Li, Y. T. Long and H. Tian, *J. Mater. Chem.*, 2011, **21**, 6054–6062.
- 63 J. Liu, K. Wang, F. Xu, Z. Tang, W. Zheng, J. Zhang, C. Li, T. Yu and X. You, *Tetrahedron Lett.*, 2011, **52**, 6492–6496.
- 64 K. Hara, Z. S. Wang, T. Sato, A. Furube, R. Katoh, H. Sugihara, Y. Dan-oh, C. Kasada, A. Shinpo and S. Suga, *J. Phys. Chem. B*, 2005, **109**, 15476–15482.
- 65 K. Hara, T. Sato, R. Katoh, A. Furube, Y. Ohga, A. Shinpo, S. Suga, K. Sayama, H. Sugihara and H. Arakawa, *J. Phys. Chem. B*, 2003, **107**, 597–606.
- 66 Z. S. Wang, Y. Cui, K. Hara, Y. Dan-oh, C. Kasada and A. Shinpo, *Adv. Mater.*, 2007, **19**, 1138–1141.
- 67 Z. S. Wang, Y. Cui, Y. Dan-oh, C. Kasada, A. Shinpo and K. Hara, *J. Phys. Chem. C*, 2008, **112**, 17011–17017.
- 68 S. Huang, Y. Hsu, Y. Yen, H. H. Chou, J. T. Lin, C. Chang, C. Hsu, C. Tsai and D. Yin, *J. Phys. Chem. C*, 2008, **112**, 19739–19747.
- 69 D. P. Hagberg, T. Edvinsson, T. Marinado, G. Boschloo, A. Hagfeldt and L. Sun, *Chem. Commun.*, 2006, 2245–2247.
- 70 K. R. J. Thomas, J. T. Lin, Y. Hsu and K. Ho, *Chem. Commun.*, 2005, 4098–4100.
- 71 H. N. Tian, X. C. Yang, R. K. Chen, R. Zhang, A. Hagfeldt and L. C. Sun, *J. Phys. Chem. C*, 2008, **112**, 11023–11033.
- 72 W. H. Liu, I. C. Wu, C. H. Lai, C. H. Lai, P. T. Chou, Y. T. Li, C. L. Chen, Y. Y. Hsu and Y. Chi, *Chem. Commun.*, 2008, 5152–5154.
- 73 B. S. Chen, D. Y. Chen, C. L. Chen, C. W. Hsu, H. C. Hsu, K. L. Wu, S. H. Liu, P. T. Chou and Y. Chi, *J. Mater. Chem.*, 2011, **21**, 1937–1945.
- 74 M. B. Smith and J. March, *March's Advanced Organic Chemistry: Reactions, Mechanisms, and Structure*, John Wiley & Sons, Inc., 5th edn, 2001, p. 684.
- 75 D. Y. Chen, Y. Y. Hsu, H. C. Hsu, B. S. Chen, Y. T. Lee, H. S. Fu, M. W. Chung, S. H. Liu, H. C. Chen, Y. Chi and P. T. Chou, *Chem. Commun.*, 2010, **46**, 5256–5258.
- 76 S. Wang, J. Guo, Y. Deng, J. Zhao and L. Zhang, *J. Mater. Sci.*, 2012, **47**, 1843–1851.